

Article

Selective Non-steroidal Glucocorticoid Receptor Modulators for the Inhaled Treatment of Pulmonary Diseases

Martin Hemmerling, Stinabritt Nilsson, Karl Edman, Stefan Eirefelt, Wayne Russell, Ramon Hendrickx, Eskil Johnsson, Carina Kärrman-Mårdh, Markus Berger, Hartmut Rehwinkel, Anna Abrahamsson, Jan Dahm, Anders R. Eriksson, Balint Gabos, Krister Henriksson, Nafizal Hossain, Svetlana Ivanova, Anne-Helene Jansson, Tina J. Jensen, Anders Jerre, Henrik Johansson, Tomas Klingstedt, Matti Lepistö, Martin Lindsjö, Irene Mile, Grigorios Nikitidis, John Steele, Ulrika Tehler, Lisa Wissler, and Thomas Hansson

J. Med. Chem., **Just Accepted Manuscript** • DOI: 10.1021/acs.jmedchem.7b01215 • Publication Date (Web): 22 Sep 2017

Downloaded from <http://pubs.acs.org> on September 23, 2017

Just Accepted

“Just Accepted” manuscripts have been peer-reviewed and accepted for publication. They are posted online prior to technical editing, formatting for publication and author proofing. The American Chemical Society provides “Just Accepted” as a free service to the research community to expedite the dissemination of scientific material as soon as possible after acceptance. “Just Accepted” manuscripts appear in full in PDF format accompanied by an HTML abstract. “Just Accepted” manuscripts have been fully peer reviewed, but should not be considered the official version of record. They are accessible to all readers and citable by the Digital Object Identifier (DOI®). “Just Accepted” is an optional service offered to authors. Therefore, the “Just Accepted” Web site may not include all articles that will be published in the journal. After a manuscript is technically edited and formatted, it will be removed from the “Just Accepted” Web site and published as an ASAP article. Note that technical editing may introduce minor changes to the manuscript text and/or graphics which could affect content, and all legal disclaimers and ethical guidelines that apply to the journal pertain. ACS cannot be held responsible for errors or consequences arising from the use of information contained in these “Just Accepted” manuscripts.

1
2
3
4
5
6
7
8
9
10
11
12
13
14
15
16
17
18
19
20
21
22
23
24
25
26
27
28
29
30
31
32
33
34
35
36
37
38
39
40
41
42
43
44
45
46
47
48
49
50
51
52
53
54
55
56
57
58
59
60

	Pharmaceutical Sciences Wissler, Lisa; PEPPAREDSLEDEN 1, Hansson, Thomas; Medicines for Malaria Venture; AstraZeneca AB

SCHOLARONE™
Manuscripts

Selective Non-steroidal Glucocorticoid Receptor Modulators for the Inhaled Treatment of Pulmonary Diseases

Martin Hemmerling,^{*†} Stinabritt Nilsson,^Δ Karl Edman,[‡] Stefan Eirefelt,^Δ Wayne Russell,^Δ
Ramon Hendrickx,[†] Eskil Johnsson,[†] Carina Kärrman Mårdh,[†] Markus Berger,[#] Hartmut
Rehwinkel,[#] Anna Abrahamsson,[†] Jan Dahmén,^Δ Anders R. Eriksson,[†] Balint Gabos,^Δ Krister
Henriksson,^Δ Nafizal Hossain,^Δ Svetlana Ivanova,^Δ Anne-Helene Jansson,^Δ Tina J. Jensen,[†]
Anders Jerre,^Δ Henrik Johansson,^Δ Tomas Klingstedt,^Δ Matti Lepistö,[†] Martin Lindsjö,[¶] Irene
Mile,^Δ Grigorios Nikitidis,^Δ John Steele,[†] Ulrika Tehler,[¶] Lisa Wissler,[‡] and Thomas
Hansson[†]

[†]Respiratory, Inflammation & Autoimmunity, Innovative Medicines and Early Development Biotech
Unit, AstraZeneca, Pepparedsleden 1, Mölndal 43183, SE

[‡]Discovery Sciences, Innovative Medicines and Early Development Biotech Unit, AstraZeneca,
Pepparedsleden 1, Mölndal 431 83, SE

[¶]Pharmaceutical Sciences, Innovative Medicines and Early Development Biotech Unit, AstraZeneca,
Pepparedsleden 1, Mölndal 43183, SE

[#]Medicinal Chemistry Berlin, Drug Discovery, Pharmaceuticals, Bayer AG, Berlin 13353, DE

^ΔAstraZeneca R&D Lund, Scheelevägen 1, Lund 22187, Sweden, SE

ABSTRACT

A class of potent, non-steroidal, selective indazole ether based glucocorticoid receptor modulators (SGRMs) was developed for the inhaled treatment of respiratory diseases. Starting from an orally available compound with demonstrated anti-inflammatory activity in rat, a soft drug strategy was implemented to ensure rapid elimination of drug candidates and minimize systemic GR activation. The first clinical candidate **1b** (AZD5423) displayed potent inhibition of lung edema in a rat model of allergic airway inflammation following dry powder inhalation combined with a moderate systemic GR-effect, assessed as thymic involution. Further optimization of inhaled drug properties provided a second, equally potent, candidate **15m** (AZD7594) that demonstrated an improved therapeutic ratio over the benchmark inhaled corticosteroid **3** (fluticasone propionate) and prolonged inhibition of lung edema, indicating potential for once-daily treatment.

INTRODUCTION

In 1948 the introduction of glucocorticoids (GCs) into clinical practice constituted a breakthrough in anti-inflammatory therapy.¹ Further developments led to synthetic steroids with improved therapeutic profiles that are, to date, the mainstay of inflammatory and autoimmune disease therapy.² GCs act through binding to the glucocorticoid receptor (GR), triggering the up- and down-regulation of gene transcription and ultimately modulation of the immune response and energy homeostasis.³ The latter GR function is associated with clinical adverse effects and limits the prolonged use of traditional steroidal GR agonists.⁴ The search for glucocorticoids with reduced adverse effects led to the discovery of non-steroidal GR modulators, which have the potential to dissociate the desired anti-inflammatory activity from metabolic adverse effects at a mechanistic level through differential DNA binding and co-regulator recruitment. For pulmonary diseases such as asthma and chronic obstructive

pulmonary disease (COPD), an inhalation approach may limit systemically driven adverse effects.⁵ Whilst inhalation delivery effectively reduces circulating drug levels, chronic treatment with inhaled corticosteroids (ICS) can still lead to suppression of the hypothalamic-pituitary-adrenal (HPA) axis, an indicator of systemic GR activation.⁶ Documented adverse effects associated with ICS include growth retardation in children, bone mineral loss and development of type II diabetes in the elderly population.⁷ In addition, patients with severe asthma and COPD often exhibit reduced responsiveness to current ICS therapy and more efficacious alternatives are highly anticipated.⁸ Herein we describe the medicinal chemistry program leading to the discovery of two inhaled non-steroidal clinical drug candidates, **1b** and **15m**, aimed at the control of pulmonary diseases with an inflammatory component such as asthma and COPD.

We recently reported the discovery of indazole ethers as a novel class of highly potent non-steroidal GR modulators covering a wide range of the physicochemical property space and thus with the potential to be optimized for different routes of administration.⁹

In this series, compound **1a** demonstrated excellent oral efficacy in a rat arthritis model but also exhibited several properties consistent with the inhalation design guidelines for pulmonary targeting *via* inhaled administration.¹⁰ Overall, **1a** possesses suitable solid state properties such as crystallinity and low hygroscopicity to facilitate dry powder inhalation (DPI) formulations. More specifically, **1a** displayed picomolar cellular potency (transrepression activity) in a range similar to current ICS (Figure 1), preferred to overcome dose limitations set by the device capacity.¹¹ In addition, compound **1a** exhibited high nonspecific binding to rat plasma protein (99.99 % bound) coupled to a high steady state volume of distribution in rat (V_{ss} 13.5 L/kg).⁹ As large volumes result when nonspecific binding to lipids exceeds the nonspecific binding to plasma protein,¹² it was hypothesized that high tissue affinity would contribute to increased local drug levels following inhalation. We

concluded that compound **1a** was a suitable starting point for a chemistry program to identify an inhaled, selective non-steroidal GR modulator (SGRM) to provide a safer treatment of asthma than current ICS. For the preclinical evaluation, a preceded methodology was adopted to assess the therapeutic ratio in the rat, derived from the inhibition of allergen-induced lung edema and the systemic involuting effect on the thymus.¹³

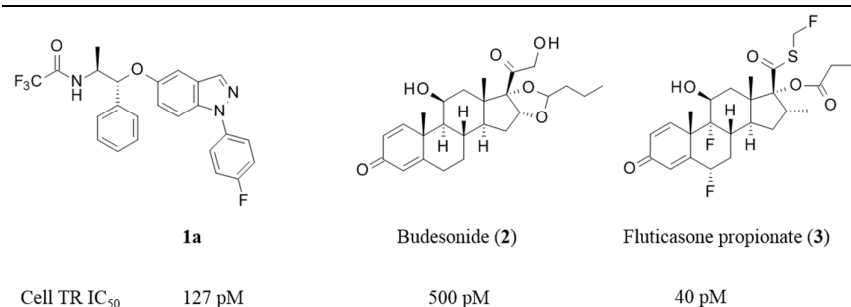


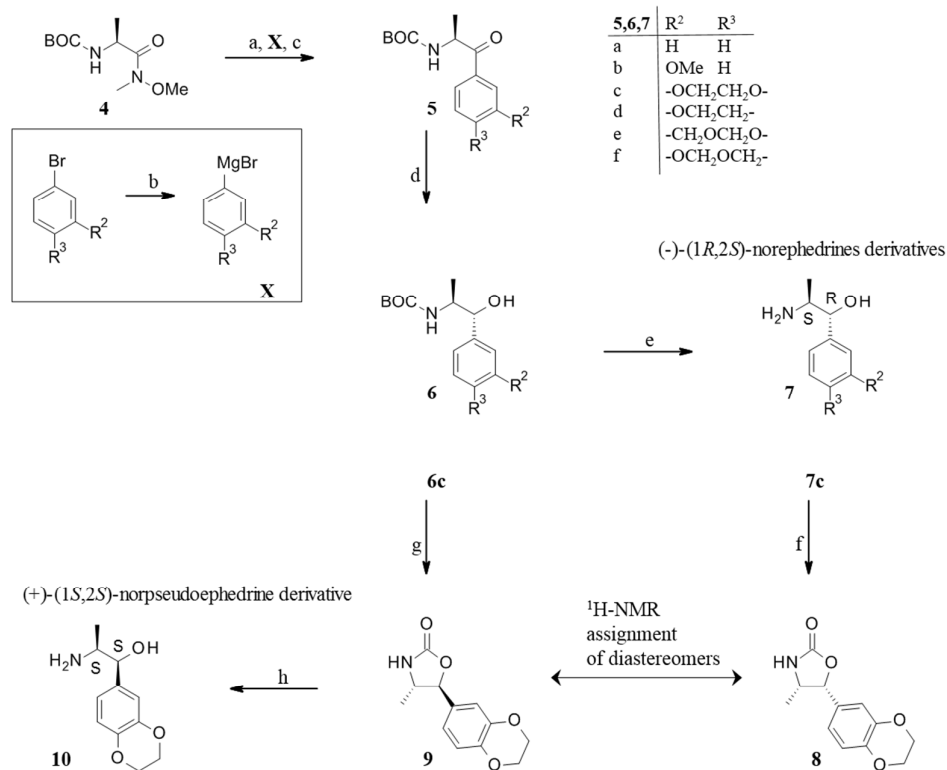
Figure 1: GR ligands with picomolar transrepression potency

CHEMISTRY

The general synthetic strategy for the indazole series follows the route outlined in Schemes 1 and 2. To facilitate a building block approach, the basic indazole ether core was assembled by an ether formation, fusing a 5-iodo-indazole with a substituted norephedrine **7**. The modified norephedrines were available through the Weinreb-Nahm ketone synthesis reacting the Weinreb amide of a suitably protected L-alanine derivative (**4**) with a freshly-prepared aryl-Grignard reagent to form the phenylalkyl ketone **5**.¹⁴ A stereoselective Meerwein-Ponndorf-Verley reduction¹⁵ provided the carbamoyl-protected substituted norephedrines **6** as single stereoisomers that following deprotection yielded the corresponding (1*R*,2*S*)-norephedrines **7** having the same absolute configuration as natural (-)-norephedrine. The enantiomers with (1*S*,2*R*)-configuration are accessible from D-alanine applying the same diastereoselective route. Specific rotations obtained for the (1*R*,2*S*) intermediate **7c** were similar to the reported value for (-)-norephedrine¹⁶, supporting the assignment of absolute

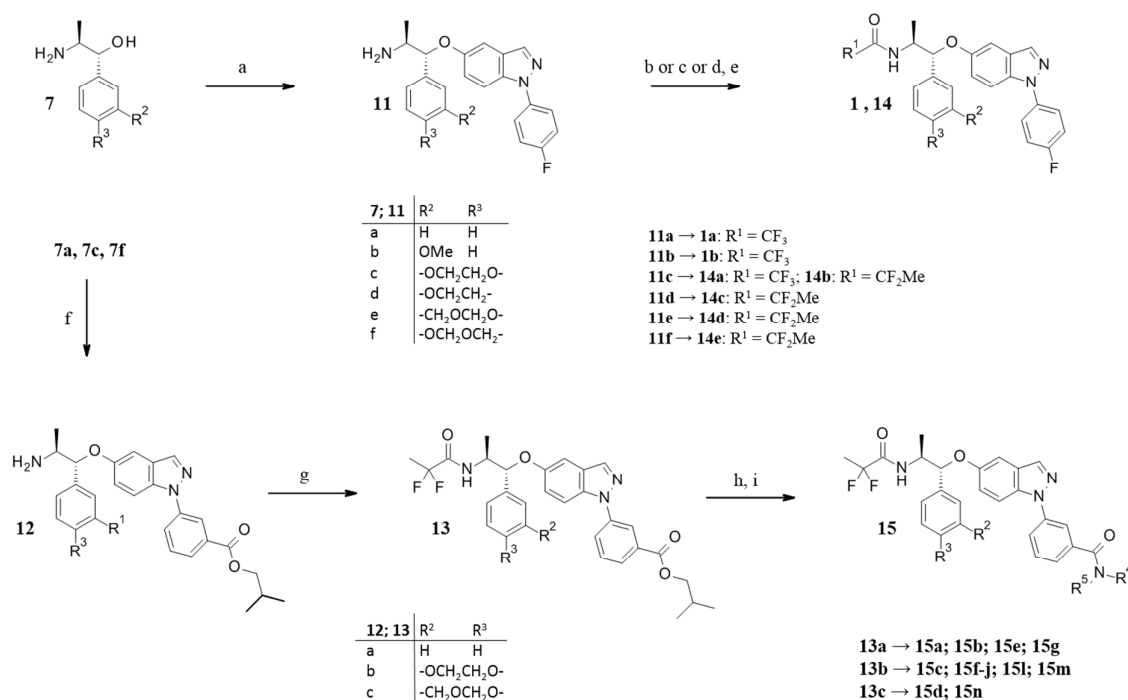
configuration. The opposite, positive rotation was measured for the (1*S*,2*R*) enantiomer **ent-7c**. To access the *syn*-diastereomers with (*S,S*) and (*R,R*) configuration, a published method was applied to transform the *tert*-butyl carbamoyl-protected amino alcohols in **6c** to 4-methyl-5-aryl-substituted oxazolidine-2-one **9** with concomitant inversion of the benzylic stereocenter.¹⁶ Proton NMR comparison with the 4,5-*cis*-substituted oxazolidin-2-one **8**, formed with conservation of both stereocenters, confirmed the relative configuration of the diastereomers. Hydrolysis of the oxazolidinone with retention of stereoconfiguration released the norpseudoephedrine **10**. The final steps to the putative GR-ligands are shown in Scheme 2. The indazole ether core was synthesized by an Ullmann coupling of a substituted norephedrine **7** and an iodoindazole to produce the primary amine intermediates **11** and **12**.¹⁷ Further conversion to carboxamides using standard amide coupling conditions provided the final indazole ether ligands **1** and **14** or the isobutyl ester intermediate **13**. Saponification and a second amide coupling yielded the extended indazole ether ligands **15**.

Scheme 1: Diastereoselective synthesis of phenylpropanolamine analogues



Reagents and conditions: a) $i\text{-PrMgCl} \cdot \text{LiCl}$, 0-10°C; b) $i\text{-PrMgCl}$, THF, 0°C – rt; c) aq. HCl (1.5 N), EtOAc, 10 °C; d) $\text{Al}(\text{OiPr})_3$ (0.2 equiv.), $i\text{-PrOH}$ (11 equiv.), toluene, 50°C; e) HCl; f) triphosgene, THF, -15 °C to rt; g) MeSO_2Cl , Et_3N , THF, 50 °C; h) LiOH, THF/ H_2O , 90 °C.

Scheme 2: Synthesis of indazole ethers



For specified substituents NR⁴R⁵ refer to Table 2. Reagents and conditions: a) 1-(4-fluorophenyl)-5-iodo-indazole (**16**), CuI (0.05 equiv.), Cs₂CO₃ (2.2 equiv.), *n*-PrCN, 125 °C; b) [R¹C(O)]₂O; NEt₃; c) R¹CO₂H, NEt₃, T3P, MeCN; d) (acetoxy)acylchloride, DIPEA, THF; e) NH₄OH, MeOH; f) isobutyl 3-(5-iodoindazol-1-yl)benzoate (**17**), CuI (0.05 equiv.) Cs₂CO₃ (2.2 equiv.), *n*-PrCN, 110 °C; g) 2,2-difluoropropionic acid, HATU, DIPEA, DCM; h) LiOH, THF/H₂O (1:1); i) HNR⁴R⁵, HBTU, DIPEA, DMF.

RESULTS AND DISCUSSION

Inhaled administration of GR modulators aims to minimize adverse effects, and the improved safety profile of current marketed agents is largely attributable to reduced systemic concentrations compared to oral treatment.^{7a} However, once absorbed into the systemic circulation, rapid inactivation is important to reduce the risk of side effects. The most-prescribed ICS are all antedugs where metabolically labile motifs are appended to the otherwise stable steroidal core.^{10a} Three prominent examples, budesonide (**2**), fluticasone propionate (**3**) and fluticasone furoate, achieve hepatic deactivation through oxidative

degradation of labile substituents at the 16α , 17α or 17β position of the familiar tetracyclic steroid core¹⁸ and a similar strategy was considered for the evolution of the starting point **1a** which was characterized by high resistance to hepatic degradation and high systemic stability.⁹ Analysis of the binding conformation of **1a** and **2** reveals that parts of the indazole ether scaffold superimpose, or are in close proximity with the substituents of the steroidal positions 17 and 16 (Figure 2). From a design perspective, it was plausible to introduce metabolically labile substituents either as modified amide residues, or in the meta- and para-positions of the norephedrine aryl group, designed to mimic the 17β -group and the $16\alpha, 17\alpha$ -group respectively. The metabolic clearance was assessed in human hepatocytes, with the resulting data used for prediction of *in vivo* hepatic extraction.¹⁹

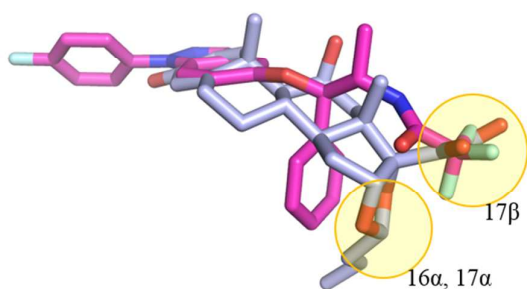


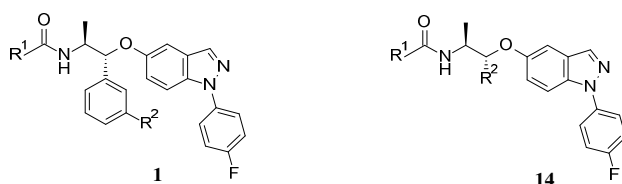
Figure 2: Superimposition of the GR complexes of **1a** (magenta) and **2** (blue); protein not shown (RMSD 0.44 for 984 main chain atoms). Steroid sites with precedent for metabolic deactivation are marked with yellow circles.

Designing in metabolic lability needed to be achieved within the established SAR of GR agonism, as subnanomolar potency is commonplace for commercial ICS. To this end it was critical to monitor potency and also crystallinity of the new ligands, since both properties play a pivotal role in successful inhaled delivery and efficacy. Cellular potency was assessed both

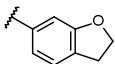
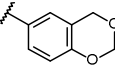
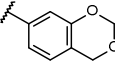
as repression of AP-1 dependent transcription (Cell TR) and as inhibition of LPS-stimulated TNF- α production in human peripheral blood mononuclear cells (PBMC).

The first metabolic inactivation option, the introduction of amides, was limited by the structure-activity relationship of the series. As reported in a recent study on the indazole ether series, small substituents including cyclopropyl, *tert*-butyl and trifluoromethyl amides with low conversion in hepatocytes were preferred for potency.⁹ Therefore, the plan to achieve metabolic inactivation focused on the exploration of the norephedrine phenyl moiety where lipophilic extensions were well tolerated.

Table 1. *In vitro* properties of *N*-fluoro-phenyl indazole ethers in comparison with the ICS 2 and 3



Cpd	R ¹	R ²	Cell TR ^{a,b}		Human PBMC ^{a,d}		Human hepatic clearance ^e		DSC ^f mp (°C)	Chrom logD
			IC ₅₀ (nM)	Eff. (%) ^c	IC ₅₀ (nM)	Eff. (%) ^c	<i>in vitro</i> CL _{int}	<i>in vivo</i> E _H		
1a	CF ₃	H	0.13 ±0.003 (2)	92	0.50 ±0.27 (2)	83	<2.1	<0.2	121	6.1
1b	CF ₃	MeO	0.049 ±0.019 (2)	114	0.16 ±0.10 (6)	82	16	0.7	82	6.0
1c	CF ₃	OH	8.00 ±3.28 (2)	122	4.60 ±5.50 (9)	82	33	0.8	NA	5.0
1d	CF ₃	OS(O) ₂ OH	464 ±255 (3)	89	NT	-	<2.7	0.3	NA	(ClogP 3.7)
14a	CF ₃		0.029 ±0.014 (2)	105	0.073 ±0.075 (6)	83	NT	-	NA	5.7
14b	MeCF ₂		0.020 ±0.002 (2)	121	0.080 ±0.015 (2)	84	28	0.8	117	5.5

14c	MeCF ₂		0.032 ±0.002 (2)	108	0.101 ±0.016 (2)	87	14	0.6	121	5.7
14d	MeCF ₂		0.156 ±0.11 (2)	117	0.322 ±0.10 (4)	70	20	0.7	NA	5.4
14e	MeCF ₂		0.066 ±0.024 (2)	114	0.132 ±0.004 (3)	67	15	0.7	NA	5.4
2			0.50 ±0.23 (6)	111	1.57 ±0.94 (12)	79	20	0.7	255	3.4
3			0.040 ±0.002 (8)	113	0.044 ±0.045 (9)	85	33	0.8	280	4.9

^aValue as mean ±SD (number of replicates). ^bTransrepression activity (TR), assessed as inhibition of AP-1 mediated transcription. ^cEfficacy, maximum response relative to Dexamethasone (100 %). ^dLPS-induced TNF-α release in peripheral blood mononuclear cells (PBMCs). ^eThe intrinsic clearance (Cl_{int} ; μL/min/10⁶ cells) in human hepatocytes was scaled to give an estimate for the *in vivo* hepatic clearance and the extraction ratio (E_H) at hepatic blood flow of 20 mL/min/kg. ^fMelting point of crystalline material only, assessed by differential scanning calorimetry. NA, not applicable. NT, not tested.

This alternative approach built on the introduction of a metabolically labile methoxy group to the norephedrine phenyl. An anisole derivative was expected to be metabolically stable in organ tissue but could serve as a substrate for cytochrome-mediated degradation in the liver. In principle, oxidative demethylation and subsequent conjugation of the resulting phenol by secondary metabolism should render compounds inactive at the GR. In practice, the introduction of a methoxy group provided compound **1b** which combined excellent potency in both the reporter gene cell assay and in human PBMCs with rapid conversion in hepatocytes, corresponding to a predicted extraction in man of 67% of liver blood flow (Table 1).

Summarizing this initial effort to tailor the properties of the lead compound **1a**, few examples were found that met the *in vitro* requirements for functional cellular potency combined with

rapid degradation in hepatocytes. Between these **1b** was the only compound that could be crystallized (mp 82 °C), indicating the potential for dry powder inhalation. The systemic rat pharmacokinetics of compound **1b** indicated that the clearance from circulation (CL 38 mL/min/kg) was well predicted from clearance in rat hepatocytes. The large volume of distribution V_{ss} (23 L/kg) indicated a high tissue affinity of **1b** and led to an extended terminal half-life of 4.7 hours. A high fraction of the oral dose was absorbed from the gastrointestinal tract and led to a moderate oral bioavailability of 37 % (Table 4).

To validate the soft-drug principle the metabolic fate of **1b** was studied in hepatocytes from different species. In human and dog hepatocytes the GR-inactive sulfate **1d** was the only major metabolite, suggesting that efficient deactivation of **1b** could be achieved. However, in rat hepatocytes the active phenol **1c** (rat PBMC IC_{50} 0.56 nM) was predominantly formed and is expected to provide a minor contribution to the systemic GR activity in the rat but not in dog or man (Supplementary Information, Scheme S1).

Having demonstrated satisfactory plasma pharmacokinetics, the inhalation properties of **1b** were investigated in advanced dry powder inhalation systems which allow for pulmonary particle distribution by active breathing.²⁰ A delayed distribution into the systemic circulation is desirable to prolong the pulmonary residence time of the drug to favor the local over systemic effects.^{10a, 10d, 21} In our hands, the mean retention times (MRT) in rat lung for established ICS were found to be 0.74 to 6.5 hours for **2** and **3** respectively. Inhaled **1b** displayed a mean retention time of 1.5 hours, similar to the faster absorbed **2** (Table 5) which supported further evaluation of its anti-inflammatory efficacy in a rat PD model of allergic asthma.²² Following dry powder inhalation **1b** potently inhibited Sephadex-induced lung edema in a dose-dependent manner with an ED_{50} of 1.2 μ g/kg, 4-fold more potent than the comparator **3** in this model (Table 6).

As a sensitive marker of systemic GR agonism, thymic involution was evaluated in the same Sephadex-challenged animals, measured as an ED₂₅ value: reduction of thymus weight by 25%.²³ In this model, both **1b** and **3** exerted a similar effect on thymus weight. Thus, **1b** displayed a 4-5-fold improvement in therapeutic ratio (TR) in rat over the benchmark ICS **3** when using the formula TR = ED₂₅ thymus involution / ED₅₀ lung edema (Table 6).

We therefore decided to nominate **1b** for clinical evaluation in asthma patients as a development candidate drug, 2,2,2-trifluoro-*N*-((1*R*,2*S*)-1-((1-(4-fluorophenyl)-1*H*-indazol-5-yl)oxy)-1-(3-methoxyphenyl)propan-2-yl)acetamide (AZD5423).²⁴

With **1b** progressing into clinical studies, a follow up program set out to expand the indazole ether series and deliver a second candidate drug. The key achievements of **1b**, in particular picomolar cellular potency and efficient deactivation in human hepatocytes, needed to be retained but there was still scope to improve the lung retention. A compound with slower distribution from lung to circulation could provide two benefits. First, a reduction in peak systemic drug levels and second, an extended duration of efficacy in lung tissue, thereby providing a once-daily dosing platform. An additional design ambition was to avoid active rat metabolites and thereby simplify the efficacy and safety evaluations.

The first modifications of **1b** built on the methoxyphenyl motif which provided the rat-specific phenol metabolite **1c**. Guided by previous indazole ether SAR, electron-rich bicyclic residues (R² in **14**, Table 1) were expected to maintain high potency. Annulation into a cyclic ether motif would preserve the metabolically-labile site, as hepatic degradation would be expected to occur α - to the ether oxygen, resulting in more polar, ring-opened metabolites with reduced GR activity.

Example **14a**, containing a *dihydro*-1,4-benzodioxane R² group, showed a modest two-fold increase in potency over the first candidate **1b** in both of the cellular transrepression assay and

in PBMCs. A further change from the trifluoroacetamide to the 2,2-difluoropropionamide introduced an additional dipole and provided the equipotent and crystalline **14b** and **14c** (a dihydrobenzofuran analogue). Importantly, the accelerated clearance in human hepatocytes indicated that the benzodioxane heterocycle could enhance the soft-drug potential. Use of the other isomeric and slightly more polar benzodioxanes at R^2 was less promising, giving reduced potencies and amorphous products, examples **14d** and **14e**.

Compound **14b** showed improved potency and intrinsic crystallinity compared to **1b** and was thus further profiled for rat pharmacokinetics *in vivo*. Following *iv* administration, plasma PK of the two compounds was similar, although the oral bioavailability of **14b** decreased to 11% (Table 4). Following intratracheal administration (*it*), the lung PK showed rapid absorption of **14b** with a slightly improved lung retention after 4 hours (4.5% of dose, Table 5) compared to the first candidate **1b** (1% of dose).

Although **14b** represented progress, its high lipophilicity and intrinsic crystallinity were similar to the first selected candidate **1b** and resulted in an almost identical pharmacokinetic profile. To obtain a truly differentiated drug candidate, the target profile was revised in two ways. First, to significantly delay absorption from the lung, slow dissolution driven by high crystallinity was prioritized. Secondly, an increase in polarity would reduce permeation through lung tissue, lowering the volume of distribution to reduce exposure in peripheral tissue. As more drastic structural changes would be needed to achieve this, a structure-guided approach was adopted to identify opportunities for addition of polar interactions within the GR binding pocket.

The X-ray structure of **1b** in complex with the GR LBD and a NCOA2 peptide (residues 740-753) confirmed that **1b** exploits all regions of the receptor used by traditional, steroidal glucocorticoids (Figure 3A). As such, the ligand binding pocket offers limited scope to significantly modify the chemical scaffold. However, in common with compound **1a** and

other GR ligands displaying a similar indazole motif,^{9, 25} the fluorophenyl group of **1b** rearranged the gatekeeper residues *Gln570* and *Arg611*, expanding the binding pocket between helices 3 and 5. As a result, the ligand-binding pocket is fused with a large cavity beneath *Trp577* (Figure 3B). This cavity is lined with hydrophilic residues and in the crystal structure is filled with ordered water molecules and an ethylene glycol derived from the crystallization conditions. This presented an opportunity to extend the indazole ether core to exploit the solvated cavity with new ligands of increased size and polar surface area – in line with the revised target profile. As an added benefit, the additional polar groups could facilitate intermolecular interactions in the crystalline state and consequently increase the melting point.

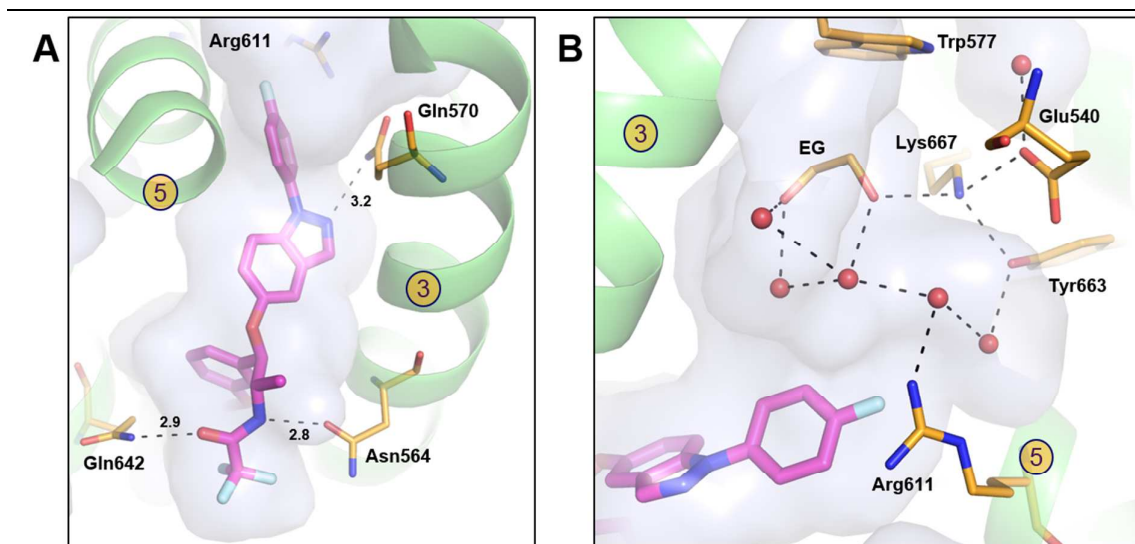
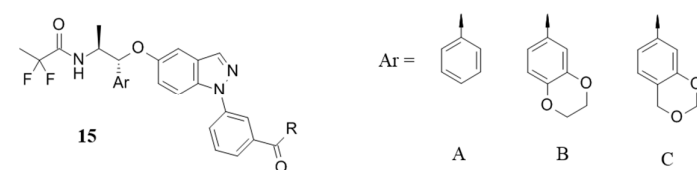


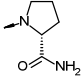
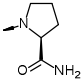
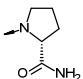
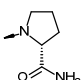
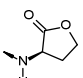
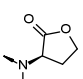
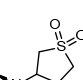
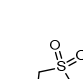
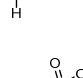
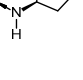
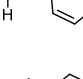
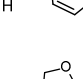
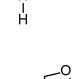
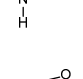
Figure 3. GR LBD (green) in complex with compound **1b** (magenta). Putative hydrogen bonds are marked with dashed lines. (A) Compound **1b** places the amide within hydrogen bonding distance of *Asn564* and *Glu642* of helices 3 and 7, respectively. The fluorophenyl motif is inserted in the induced pocket in between helices 3 and 5. (B) The meta position of the fluorophenyl motif is directed towards a large cavity beneath *Trp577*.

Based on crystallographic data, the familiar phenyl indazole moiety was extended from the meta-position of the N-phenyl group. By analogy to published GR modulators,^{25d} a carboxamide was selected as a polar linker to position side chains along the preferred vector into the induced, solvent stabilized cleft (Figure 3). Amino acid amides were initially explored as polar substituents to form amides of the general structure **15**, exemplified by the prolines **15a** to **15d** (Table 2). The D-prolinamide residue proved to be the preferred stereoisomer and excellent potency was achieved for all aryl substituents A to C. However, the reduced lipophilicity limited intrinsic clearance in hepatocytes. Furthermore, the polar prolinamide functionality increased solubility and derailed our attempts to reduce aqueous solubility by increasing crystallinity and melting point. Switching to the related γ -butyrolactone instead of a proline in **15e** and **15f** resulted in a breakthrough, providing compounds that were easily crystallized, melting in the region of 200°C - an increase of about 100°C compared to the first candidate **1b**. Importantly, for this matched pair of butyrolactones the bicyclic aryl variant B in **15f** improved potency by an order of magnitude over its partner **15e**. In human hepatocytes, **15f** was more rapidly cleared than the more-polar prolines **15c** and **15d**, reaching the target of > 60% of predicted hepatic extraction (E_H). Overall, **15f** achieved all of the *a priori* target criteria and is a key bridgehead for the design of improved analogues.

Table 2: Carboxamide extended indazole ethers



Cpd	Ar	R	Cell TR ^{a,b}		Human PBMC ^{a,d}		Human hepatic clearance ^e		DSC ^f	Solubility ^g	Chrom logD
			IC ₅₀ (nM)	Eff. (%) ^c	IC ₅₀ (nM)	Eff. (%) ^c	<i>in vitro</i> CL _{int}	<i>in vivo</i> E _H	mp (°C)	S / C (μM)	

15a	A		0.21 ±0.08 (3)	107	1.1 ±0.61(2)	78	<2.7	<0.3	A	36 / NA	3.3
15b	A		17.0 ±1.88 (2)	86	NT	NT	NT	NA	NA	85 / NA	3.3
15c	B		0.12 ±0.008 (2)	99	0.25 ±0.18 (2)	80	11	0.6	NA	47 / NA	2.9
15d	C		0.15 ±0.078 (2)	85	0.61 ±0.10 (2)	61	9.7	0.6	NA	19 / NA	2.9
15e	A		13.4 ±5.95 (2)	92	18 ±0.76 (4)	63	NT	NA	221	2.0 / 0.12	3.9
15f	B		0.92 ±0.13 (2)	101	0.93 ±0.33 (2)	66	17	0.7	183	0.16 / 0.22	3.6
15g	A		2.4 ±0.62 (2)	103	5.0 (1)	58	<2.7	<0.3	140	1.0 / 0.34	3.8
15h	B		0.21 ±0.11 (8)	99	1.4 ±0.39 (6)	69	23	0.7	180	0.01 / 0.68	3.6
15i	B		0.17 ±0.035 (10)	102	0.54 ±0.32 (8)	70	22	0.7	215	<0.01 / <0.1	3.6
15j	B		0.037 ±0.003(2)	104	0.17 ±0.041 (4)	72	21	0.7	127	<0.1 / 0.23	3.7
15k	C		0.062 ±0.055 (5)	103	0.38 ±0.23 (6)	70	21	0.7	158	<0.1 / 0.02	3.6
15l	B		0.051 ±0.004 (2)	105	0.66 ±0.038 (6)	78	30	0.8	175	1.3 / 0.09	3.7
15m	B		0.056 ±0.021 (4)	107	0.43 ±0.16 (6)	75	29	0.8	177	<0.1 / 0.02	3.7
15n	C		0.19 ±0.018 (3)	104	0.625 ±0.062 (4)	72	26	0.8	192	0.11 / 0.03	3.6

For annotations ^{a, b, c, d, e, f} refer to Table 1. ^gSolubility in 0.1M phosphate buffer (pH 7.4); S: at 20 °C, starting from 10 mM DMSO stock solution; C: at 23 °C, starting from crystalline solid. NA, not applicable. NT, not tested.

The sulfolane amides **15h** and **15i** maintained the high-melting crystalline profile and further improved potency, with a preference for the *R*-isomer in **15i**. Both isomers were rapidly cleared by human hepatocytes and compound **15i** was progressed as a potential clinical candidate for further profiling. The pyridylmethyl amide pair **15j** and **15k**, differentiated only by the regiochemistry of the norephedrine aryl group both improved on potency over the sulfolane **15i** and retained rapid clearance in hepatocytes. Whilst measured lipophilicity was similar for the regioisomeric pair, the significant difference in melting temperatures led to a very different solubility. As a result, **15j** and **15k**, provided an opportunity to study the impact of differentiated solid-state properties on *in vivo* pharmacokinetics and pharmacology, and both compounds were subjected to additional *in vivo* studies. From the triad of *N*-tetrahydrofuran-3-yl amides **15l-15n**, the epimers **15l** and **15m** could not be differentiated *in vitro*. Both compounds displayed the highest observed potencies in human and rat PBMCs and provided an increased melting point, indicating a higher intrinsic crystallinity. **15m** was arbitrarily selected for further progression. The benzodioxane regioisomer **15n** showed reduced potency and was not progressed.

As recently reported, indazole ether based GR modulators are in general highly selective.⁹ In contrast to marketed ICS that typically display nanomolar affinities at the progesterone (PR) and mineralocorticoid receptor (MR),^{10a} the indazole ether based GR modulators improve PR selectivity by at least 100-fold and show no binding to MR up to the limit of binding assay detection (Table 3). Substantially improved steroid hormone receptor selectivity could

potentially contribute to clinical safety and differentiates selective GR modulators from conventional steroids.²⁶

Table 3. Hormone receptor selectivity^{a, b}

Cpd	GR (μM)	PR (μM)	MR (μM)	AR (μM)	ERα (μM)	ERβ (μM)
1b	0.0009 ±0.0002 (2)	1.76 ±0.63 (3)	>5 (7)	>10 (4)	>10 (3)	>10 (3)
15i	0.0015 ±0.0005 (5)	>10 (5)	>10 (6)	>10 (4)	>10 (4)	>10 (4)
15j	0.0010 ±0.0011 (6)	8.28 ±1.45 (3)	>10 (3)	>10 (3)	>10 (2)	>10 (2)
15k	0.0008 ±0.0001 (6)	>10 (6)	>10 (7)	>10 (6)	>10 (6)	>10 (6)
15m	0.0009 ±0.0007 (3)	>10 (3)	>10 (3)	>10 (3)	>10 (2)	>10 (2)
2	0.0038 ^c (±0.0019) n=7	0.028 ±0.0065 (6)	0.014 ±0.010 (6)	0.71 ±0.17 (4)	>10 (3)	>10 (3)
3	0.0009 ±0.0009 (333)	0.021 ±0.014 (6)	0.149 ±0.166 (4)	>10 (3)	>10 (3)	>10 (3)
FF	0.0008 ±0.0003 (5)	0.021 ±0.007 (4)	0.166 ±0.016 (2)	1.88 ±0.28 (2)	>5 (2)	>5 (2)

^avalues as mean ± SD (number of replicates). ^bfor assay descriptions refer to the Supplementary Information. ^cassessed in Fluorescence Polarization assay format. FF; fluticasone furoate.

The primary goal of the follow up program was to identify a candidate with a differentiated PK profile leading to improved lung targeting. For the shortlisted examples of the subseries **15**, rapid clearance from circulation was similar to that observed for the first drug candidate **1b**. Furthermore, compounds **15i – 15m** demonstrated much reduced volumes of distribution (V_{ss}), shortening half-lives substantially. Most critically, the significant bioavailability observed for **1b** did not translate to **15i – 15m**, confirming that this subclass did have improved PK properties, resulting in reduced systemic exposure (Table 4).

Table 4. Plasma PK in rat^a

Cpd	Rat Hep CL _{int}	Pred. <i>in vivo</i> CL ^b	CL [iv]	V _{ss} [iv]	t _{1/2} [iv]	F [po]
	(μL/min/10 ⁶ cells)	(mL/min/kg)	(mL/min/kg)	L/kg	(h)	(%)
1b	13	34	38	23	4.7	37
14b	22	43	42	10	7.4	11
15i	31	48	102	2.8	0.3	<0.1
15j	25	45	68	0.97	0.2	0.16
15k	25	45	73	0.81	0.1	0.3
15m	34	50	30	0.16	0.1	<0.1
3	28	46	103	31	3.3	<0.1

^aMale Han Wistar rat; ^bPredicted hepatic clearance in the rat, based on intrinsic clearance in rat hepatocytes¹⁹

For all selected examples with the generic structure **15**, the combined analysis of the pharmacokinetic profiles after intravenous and inhaled administration indicated an absorption rate-limited elimination.^{7a, 10d} This was demonstrated by the prolonged terminal lung half-lives observed after DPI (Table 5), which were invariably 1-2 orders of magnitude larger than the corresponding plasma half-lives obtained after *iv* administration (Table 4). The underlying mechanism is likely a dissolution-limited absorption, because experimental solubility in human intestinal fluid (HIF), rather than lipophilicity, correlates with the observed lung retention (MRT) (Table 5). Slow particle dissolution, particularly in the less-perfused regions of the central lung, was previously shown to drive a favorable concentration gradient from the lung epithelium to the circulation, improving the lung selectivity.²⁷

The lipophilic examples **1b** and **14b** displayed similar terminal half-lives in lung and plasma after DPI and *iv* administration respectively (Table 4 and 5). This indicates that for these compounds only a transient lung selectivity was achieved through the inhalation route.

Table 5. Inhalation PK in rat^a

Cpd	Sol [HIF] ^b	% dose in lung ^c		AUC _{0-∞} ^c	t _{1/2} ^c	MRT ^c	C _{max} [plasma]
	(μM)	at 4h (%)	at 24h (%)	(μM*h)	(h)	(h)	(nM)
1b	12	0.7	0 - 0.4	18	7.5	1.5	122
14b^d	NT	6.2	0.8	12	8.9	8.8	30
15i	0.30	93	91	5200	179	210	4.9
15j	2.1	4.1	0.18	26	4.9	2.6	21
15k	1.30	41	8.6	190	9.0	10	12
15m	0.60	73	32	740	17	23	7.4
3	0.62	43	1.9	200	4.5	6.0	24

^aDry powder inhalation; normalized lung dose 0.1 μmol/kg. ^bThermodynamic solubility in human intestinal fluid at 37°C. ^cIn total lung; t_{1/2}, apparent terminal half-life in the total lung; MRT, mean residence time. ^dit instillation of the lung dose. NT, not tested.

The inhaled anti-inflammatory potential of the compounds **15i**, **15k** and **15m** was evaluated in the rat model of Sephadex induced airway inflammation. Compound **15j** shares the generic structure **15** but displayed similar lung PK properties to the first candidate **1b** and was included to allow a pharmacological assessment of the chemotype.

Table 6. PD effects in rat model of Sephadex induced airway inflammation

Sephadex-induced airway inflammation model (rat)					
Cpd	Rat PBMC ^a	Lung edema inhibition ED ₅₀	Thymus weight involution ED ₂₅	Therapeutic ratio ED ₂₅ / ED ₅₀	Exp. n ^b
	nM (% eff.) ^c	μg/kg (CI 95%) ^d	μg/kg (CI 95%) ^d	(CI 95%) ^c	
1b	0.14 (78)	1.3 (0.30, 5.6)	4.6 (1.7, 12)	3.7 (0.64, 21)	2

15i	0.34 (95)	2.4 (0.60, 9.3)	>130 (NA)	>54 (NA)	1
15j	0.29 (92)	8.7 (4.7, 16)	12 (7.1, 19)	1.4 (0.61, 3.1)	1
15k	0.10 (100)	2.7 (0.96, 7.6)	27 (15, 46)	10 (3.0, 33)	1
15m	0.30 (95)	0.8 (0.45, 1.5)	40 (17, 92)	50 (18, 140)	1
3	0.14 (81)	6.0 (1.5, 23)	3.9 (1.9, 8.1)	0.7 (0.14, 3.1)	3

^aValue as mean of at least two experiments. ^bnumber of experiments; each experiment included a minimum of 18 treated animals, divided between 3-7 dose groups with at least 4 animals in each dose group, and 12-20 untreated animals, divided between 2 groups: native and challenged. ^cEfficacy, maximum response relative to Dexamethasone (100 %). ^dCI, 95% confidence interval.

All of the profiled indazole ethers were potent with ED₅₀ values below 10 µg/kg in the rat Sephadex PD model, comparable to, or even superior to the benchmark ICS **3**. Neither potency in rat PBMCs nor total compound levels in rat lung (AUC) would predict the same efficacy ranking as observed in the PD model, which is likely to be a complex result of these and additional parameters. However, the systemic GR effect, measured by thymus involution, correlated with peak levels of total drug in blood (Table 5 and 6). As a consequence, the observed therapeutic ratio (TR) is largely dominated by the lung retention of the drug. Based on the results obtained in the rat Sephadex model, the pyridylmethyl amide ligands (**15j**, **15k**) were parked due to inferior potency and therapeutic ratio. Nonetheless, this matched pair with very similar molecular, structural and *in vitro* pharmacological properties demonstrated that divergent solid-state properties do translate into differentiated inhalation PK and PD. Ultimately, **15i** which displayed the highest therapeutic ratio was discarded in favor of **15m** which most efficiently inhibited rat lung edema. This selection was driven by a theoretical safety risk of **15i** associated with long retention exceeding 24 hours in lung of

presumably undissolved material that could be compounded by repeat dosing. The therapeutic ratio obtained was 70-fold higher for **15m** than for **3**. The experimental settings presented here do not allow a differentiation between the pharmacokinetic and mechanistic drivers of the observed therapeutic ratio.

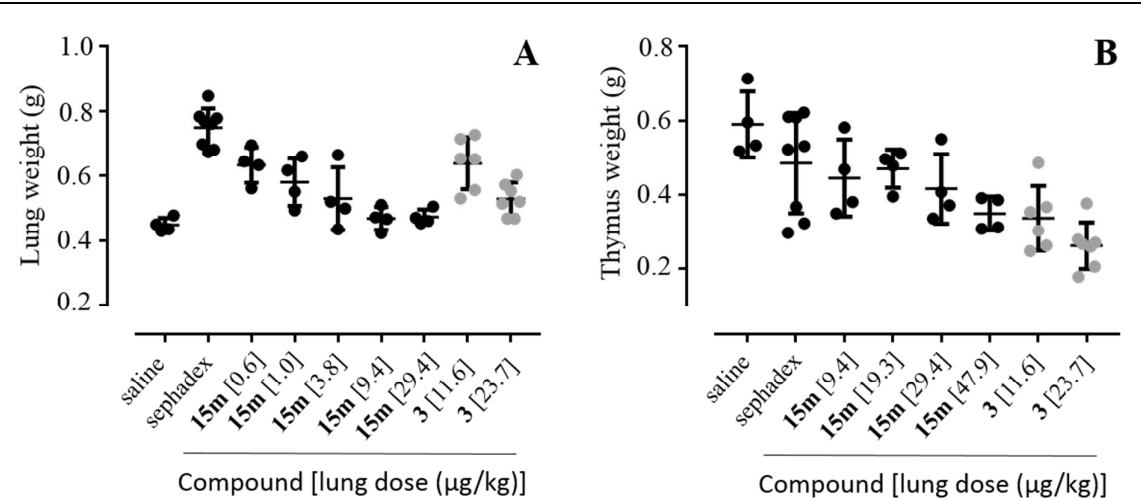


Figure 4. Dose-response study of **15m** in a 4-day rat model of Sephadex-induced airway inflammation. The anti-inflammatory effect was assessed as inhibition of the induced lung edema, determined as reduction of left lung lobe weight (A). The systemic GR agonism was assessed as thymus weight reduction (involution) in the same animals (B). The data points shown represent single animals, the bars indicate the mean and the standard deviation. DPI inhalation with **15m** (black dots) reduced the edema by 39% to 109% ($p<0.001$) with a significant effect already at the lowest dose (0.6 μg/kg, $p<0.002$). Significant effects of **15m** were observed on thymus weight only at the highest dose (47.9 μg/kg, $p=0.041$). Two doses of **3** (grey dots) were included as control.

The slow dissolution of inhaled **15m**, resulting in slow absorption into the systemic circulation, could potentially prolong the anti-inflammatory effect in the airways. To experimentally address the duration of the effect, the Sephadex rat PD model was modified in two ways. The time span between administration of the drug and Sephadex-challenge was

increased to either 9 or 24 hours to investigate the potential for once-daily treatment. This experimental design did not support multiple dosing and a single dose was given (DPI). To obtain significant results, the dose was increased to 30 $\mu\text{g}/\text{kg}$ (approx. 3-fold over ED_{90} of **15m**). As a head-to-head benchmark, an approximately equal dose of the ICS **3** was profiled in the same experiments.

Compound **15m** achieved full inhibition when pre-dosed 9 h prior to challenge and still preserved a significant effect, reducing lung edema by 76%, when dosed 24 h prior to challenge. In this model, **15m** demonstrated superiority over **3**, which showed only partial effect when pre-dosed 9 h and had no significant effect when dosed 24 h prior to challenge. The superior performance of **15m** compared with **3** is not necessarily related to the longer sustained drug release into the lung tissue but could be explained by better potency in the rat model. Nonetheless, the 10-fold lower systemic activity observed for inhaled **15m** suggests that equal or higher doses than used for **3** might be applied without increasing the risk of adverse effects.

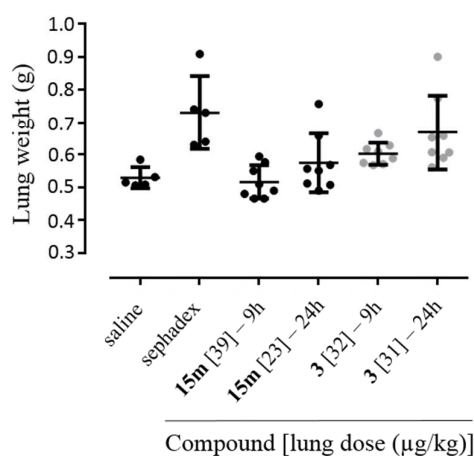


Figure 5: Duration of effect for inhibiting Sephadex-induced lung edema. **15m** (black dots) showed full inhibition effect when predosed 9 h prior to challenge ($p < 0.001$) and 76 % inhibition when dosed 24 h prior to challenge ($p < 0.001$). **3** (grey dots) inhibited the challenge-

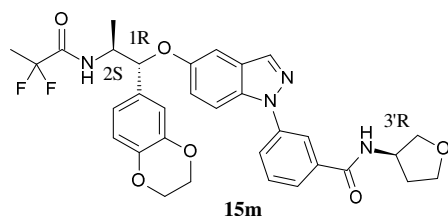
induced lung edema by 61 % when dosed 9 h prior to challenge ($p < 0.01$) but no significant inhibitory effect when dosed 24 h prior to challenge.

As compound **15m** displayed only a moderate effect on thymus size in rat, it can be concluded that the distribution of **15m** and any potential active metabolites to the thymus is less efficient compared to FP. This can be rationalized by the improved lung PK profile of **15m** which led to a slower absorption and subsequently lower plasma concentrations of the parent. In addition, the higher polarity of **15m** results in a drastically reduced volume of distribution (V_{ss} 0.16 L/kg), reducing peripheral tissue affinity. Coupled to this is the rapid clearance of **15m** from circulation by efficient degradation and elimination. To investigate the metabolic fate of the parent compound, ^{14}C -radiolabelled **15m** was prepared and profiled in human, rat and dog hepatocytes. Multiple degradation pathways were found to be active, generating a complex mixture of metabolites which was similar across the three species. Hepatic degradation proceeded predominantly by oxidation of the heterocycle of the benzodioxane moiety, followed by ring opening and glucuronidation. Another major pathway led to the cleavage of the indazole ether pharmacophore to release a 5-hydroxy-indazole fragment (Supplementary information, Table S4). Based on our understanding of the series SAR, it is very likely that GR activity is eliminated or greatly reduced in all major metabolites. Furthermore, unlike the first candidate **1b**, the risk of generating a species-specific active metabolite in a preclinical safety species was successfully mitigated. In summary, Compound **15m** combined excellent potency and a favorable therapeutic ratio in rat and was nominated as a second clinical candidate, 3-(5-((1*R*,2*S*)-2-(2,2-difluoropropanamido)-1-(2,3-dihydrobenzo[*b*][1,4]dioxin-6-yl)propoxy)-1*H*-indazol-1-yl)-*N*-((*R*)-tetrahydrofuran-3-yl)benzamide (AZD7594).²⁸

To conclude the structural investigation, the stereoisomers of candidate **15m** were prepared and tested for transrepression activity (Table 7). In the central 1-aryl-2-amino-propanoxy moiety the (1*R*,2*S*) configuration is clearly preferred, whilst the configuration of the 3-

aminotetrahydrofuran had no influence on potency. For the other stereoisomers only the *anti*-stereoisomeric pair with (1*S*,2*S*) configuration retained limited activity with the repression potency reduced by more than 100-fold.

Table 7. Transrepression activity of stereoisomers of **15m**



Cpd	15m	15l	18	19	20	21	22	23
Configuration	1 <i>R</i> ,2 <i>S</i> ,3' <i>R</i>	1 <i>R</i> ,2 <i>S</i> ,3' <i>S</i>	1 <i>S</i> ,2 <i>R</i> ,3' <i>R</i>	1 <i>S</i> ,2 <i>R</i> ,3' <i>S</i>	1 <i>S</i> ,2 <i>S</i> ,3' <i>R</i>	1 <i>S</i> ,2 <i>S</i> ,3' <i>S</i>	1 <i>R</i> ,2 <i>R</i> ,3' <i>R</i>	1 <i>R</i> ,2 <i>R</i> ,3' <i>S</i>
Cell TR IC ₅₀	0.055 ±0.021 (4)	0.051 ±0.004 (2)	>1000 (2)	>1000 (2)	12.7 ±4.0 (2)	24.3 ±5.3 (2)	>1000 (2)	>1000 (2)
%-Efficacy	107	105	6.6	9.3	100	99	35	30

Conclusion

A class of highly potent, non-steroidal GR modulators, highly selective across the steroid hormone receptor family, served as the starting point for optimization into two inhaled drug candidates for the treatment airway inflammation. Initially, a soft drug strategy was developed to ensure rapid clearance from systemic circulation. This approach delivered the first inhaled candidate **1b** which was more-rapidly absorbed than the benchmark ICS **3** (fluticasone propionate), and possessed high availability in lung tissue during the first two hours following inhaled administration to the rat. Compared to **3**, compound **1b** demonstrated marginally improved potency in inhibition of lung edema in a rat model of airway inflammation. Further optimization increased lung targeting: prolonging exposure in lung tissue whilst limiting systemic levels. A revised strategy aimed to retard drug absorption via a differentiated profile featuring decreased dissolution rate, increased polarity and increased

molecular size. This delivered the second inhalation candidate drug **15m** which achieved the requisite low solubility profile but retained the potency of the first candidate and demonstrated a robust local anti-inflammatory effect in rat lung airways at the same dose. The prolonged retention in lung tissue was balanced by limited systemic exposure, minimizing GR-driven effect on rat thymus. As a consequence, the therapeutic ratio of **15m** was increased over the first candidate **1b** and the comparator ICS **3** by an order of magnitude. Head-to-head with **3** at equivalent doses, **15m** displayed more enduring efficacy, indicating potential for once-daily dosing.

Although the development of **1b** was halted due to lack of efficacy in a phase 2 study in COPD patients,²⁹ **15m** has recently demonstrated dose-dependent efficacy in a phase 2 lung function study in asthmatics.³⁰

EXPERIMENTAL SECTION

Synthesis. *General conditions.* Commercial solvents and reagents were used without further purification. Anhydrous solvents were dried over molsieves (4Å). Water was filtered and demineralized (Milli-Q). Purification by flash chromatography was carried out using silica gel 60 (0.040-0.063 mm, Merck, or using prepacked Biotage KP-SIL or Isolute columns. Purification by HPLC was performed on a Gilson HPLC system with the following columns: Kromasil KR-100-5-C18 (250 x 20 mm), Kromasil 100-10-C18 (250 x 50 mm); gradient of acetonitrile / water (containing 0.1% TFA). Alternatively XBridge Prep C18, 5µm (150x30 mm) or XTerra Prep MS C18, 5µm (50x19 mm); gradient of acetonitrile / water containing 2 mL 28% aq. NH₄OH. In NMR spectra the chemical shifts δ are internally referenced to the residual solvent peak. Low resolution LCMS (APCI); Column Waters Symmetry C18 2.1 x 30 mm; flow: 0.7 mL/min; eluents A H₂O, B acetonitrile with both solvents containing 0.1% TFA; gradient 15% to 95% B in 2.7 min, 95% B for 0.3 min; UV detection at 254 nM. Purity was determined by HPLC: Column Kromasil C18, 5µm 3.0 x 100

mm; eluents A H₂O, B acetonitrile with both solvents containing TFA (0.1%); gradient B 10-100% in 20 min; flow 0.6 mL/min; detection at 220, 252 and 280 nm. All test compounds were of $\geq 95\%$ purity. Chiral purity was determined using the following systems: Chiral SFC: LUX Amylose-1 (AD) 3 μ m, 0.46 x 15 cm; 40% EtOH / DEA (100/0.5) in CO₂, 120 bar, 3.5 mL/min. diode array detection 215-330 nm. Chiral HPLC, method A: Chiralpak IA 5 μ m; method B: Chiralpak IB 5 μ m; both method A and B 4.6x250mm, eluent *i*-hexane / DCM / MeOH 68:30:2; flow 1 mL/min; UV=254 nm. Chiral HPLC, method C: Chiralpak IB 5 μ m, 4.6x100 mm; eluent *iso*-Hexane / DCM / MeOH / EtOH 65:29:2:4, flow 1 mL/min; UV=254 nm. Chiral HPLC, method D: Chiralpak AS-H 5 μ m, 4.6 x 50mm, eluent *i*-hexane / *i*-PrOH 95:5, flow 1 mL/min; UV=220 nm. Chiral HPLC, method E: Chiralpak AD-H 5 μ m, 4.6 x 250 mm, eluent *i*-hexane / EtOH 80:20, flow 1 mL/min, UV=220 nm.

2,2,2-Trifluoro-N-((1R,2S)-1-((1-(4-fluorophenyl)-1H-indazol-5-yl)oxy)-1-(3-methoxyphenyl)propan-2-yl)acetamide (1b). Prepared essentially as described for **13b**, starting from **11b** (21.5 g, 55 mmol), triethylamine (23 mL, 165 mmol) and trifluoroacetic anhydride (23 mL, 165 mmol). Flash chromatography on silica gel (20% EtOAc in isohexane) afforded **1b** (22.0 g, 82%) as a yellow foam. The material was crystallized from MTBE / isohexane, assisted by seed crystals, to yield **1b** as a white solid (14.0 g, 52%), mp = 82 °C. LCMS *m/z* 488 (MH⁺). $[\alpha]_D^{20}$ -44° (c 1.1, MeOH). HPLC *t*_R 14.23, >99%. ¹H NMR (600 MHz, DMSO-*d*₆) δ 9.52 (d, *J* = 8.3 Hz, 1H), 8.17 (s, 1H), 7.71 – 7.76 (m, 2H), 7.69 (d, *J* = 9.2 Hz, 1H), 7.35 – 7.42 (m, 2H), 7.26 (t, *J* = 7.9 Hz, 1H), 7.21 (dd, *J* = 2.3, 9.2 Hz, 1H), 7.13 (d, *J* = 2.3 Hz, 1H), 6.99 (d, *J* = 7.7 Hz, 1H), 6.96 (s, 1H), 6.84 (dd, *J* = 2.4, 8.2 Hz, 1H), 5.27 (d, *J* = 6.3 Hz, 1H), 4.21 – 4.3 (m, 1H), 3.72 (s, 3H), 1.33 (d, *J* = 6.8 Hz, 3H). ¹³C NMR (151 MHz, DMSO-*d*₆) δ 160.20 (d, *J* = 243.6 Hz), 159.10, 155.50 (q, *J* = 36.3 Hz), 152.74, 139.66, 136.07 (d, *J* = 2.6 Hz), 135.01, 134.09, 129.41, 125.26, 123.92 (d, *J* = 8.5 Hz), 119.83, 118.91, 116.34 (d, *J* = 22.8 Hz), 115.79 (q, *J* = 288.4 Hz), 113.15, 112.46, 111.41, 104.21,

81.23, 54.89, 50.68, 15.15. Chiral HPLC (method E) t_R = 5.5 min, 100% (1*R*,2*S* enantiomer), t_R = 7.1 min, 0% (1*S*,2*R*-enantiomer). Chiral Purity >99.9 % ee.

(*S*)-*Tert*-butyl 1-(3-methoxyphenyl)-1-oxopropan-2-ylcarbamate (**5b**). Essentially prepared as described for **5c**, starting from (3-methoxyphenyl)magnesium bromide, 1M in THF (276 mL, 276 mmol). Yield after recrystallisation from methyl *tert*-butyl ether (490 mL) 58.9 g (84%) as a colorless crystalline solid. LCMS m/z 180 (MH^+ -BOC). 1H -NMR (400 MHz, $CDCl_3$): δ 7.55 (d, J = 7.6 Hz, 1H), 7.49 (t, J = 1.9 Hz, 1H), 7.39 (t, J = 8.0 Hz, 1H), 7.15 (dd, J = 8.2, 2.0 Hz, 1H), 5.56 (d, J = 6.9 Hz, 1H), 5.28 (quint, J = 7.2 Hz, 1H), 3.86 (s, 3H), 1.47 (s, 9H), 1.41 (d, J = 7.1 Hz, 3H). Chiral HPLC (method D) t_R = 2.36 min, 99.95% (*S*-enantiomer), t_R = 1.70 min, 0.05% (*R*-enantiomer). Chiral Purity 99.9 % ee.

(*S*)-*Tert*-butyl 1-(2,3-dihydrobenzo[*b*][1,4]dioxin-6-yl)-1-oxopropan-2-ylcarbamate (**5c**). Magnesium turnings (0.46 g, 18.9 mmol) and one small iodine crystall were suspended in dry THF (3 mL) under an argon atmosphere. A solution of 6-bromo-2,3-dihydrobenzo[*b*][1,4]dioxine (4.03 g, 18.7 mmol) in dry THF (17 mL) was added. The mixture was gently heated to initiate the reaction, after a few minutes the iodine color vanished, the external heating was removed and continued stirring for one hour resulted in a green solution. GC/MS analysis of a small sample, quenched with iodine in THF, indicated a conversion of 75% of the starting bromide to the Grignard reagent to form a solution of (2,3-dihydrobenzo[*b*][1,4]dioxin-6-yl)magnesium bromide in THF (0.7 M, 20 mL, 14.0 mmol) that was used directly in next step. In a separate vessel, a suspension of (*S*)-*tert*-butyl 1-(methoxy(methyl)amino)-1-oxopropan-2-ylcarbamate (**4**) (3.0 g, 12.9 mmol) in THF (30 mL) was cooled to -15 °C and isopropyl magnesium chloride (2 M in THF, 6.5 mL, 13.0 mmol) was added keeping the temperature below -10 °C. The solid started to dissolve, the reaction temperature was allowed to reach 0 °C and the freshly prepared solution of (2,3-dihydrobenzo[*b*][1,4]dioxin-6-yl)magnesium bromide, 0.7 M in THF (20 mL, 14.0 mmol)

was added. The temperature was allowed to reach room temperature and stirring was continued for 17 h. Thereafter the reaction mixture was poured into 1N HCl (300 mL) at 10 °C, methyl *tert*-butyl ether (300 mL) was added and the mixture was transferred to a separation funnel. The water phase was extracted with methyl *tert*-butyl ether (200 mL). The ether phases were washed with water, brine and dried (Na₂SO₄). The crude product was purified by flash chromatography (MTBE / heptane 1:2) to yield **5c** as a slightly yellow sticky oil/gum (3.76 g, 95%). LCMS *m/z* 208 (MH⁺-BOC). ¹H NMR (300 MHz, DMSO-*d*₆) δ 7.50 (dd, *J* = 2.1, 8.5 Hz, 1H), 7.46 (d, *J* = 2.0 Hz, 1H), 7.23 (d, *J* = 7.5 Hz, 1H), 6.97 (d, *J* = 8.4 Hz, 1H), 4.9 – 5.03 (m, 1H), 4.24 – 4.35 (m, 4H), 1.35 (s, 9H), 1.19 (d, *J* = 7.2 Hz, 3H).

Tert-butyl (1*R*,2*S*)-1-hydroxy-1-(3-methoxyphenyl)propan-2-ylcarbamate (**6b**). Prepared as described for **6c**, starting from **5b** (17.5 g, 62.6 mmol). Yield: 17.5 g (92%). LCMS *m/z* 182 (MH⁺-BOC). ¹H NMR (300 MHz, DMSO-*d*₆) δ 7.20 (t, *J* = 8.0 Hz, 1H), 6.84 – 6.92 (m, 2H), 6.72 – 6.8 (m, 1H), 6.56 (d, *J* = 8.5 Hz, 1H), 5.27 (d, *J* = 4.7 Hz, 1H), 4.47 (t, *J* = 4.9 Hz, 1H), 3.73 (s, 3H), 3.47 – 3.63 (m, 1H), 1.31 (s, 9H), 0.94 (d, *J* = 6.7 Hz, 3H).

Tert-butyl (1*R*,2*S*)-1-(2,3-dihydrobenzo[*b*][1,4]dioxin-6-yl)-1-hydroxypropan-2-ylcarbamate (**6c**). **5c** (144 g, 469 mmol), Al(O*i*Pr)₃ (47.9 g, 235 mmol) and propan-2-ol (464 mL, 6.1 mol) in toluene (840 mL) were stirred at 50 °C under argon atmosphere for 16 h. The reaction mixture was cooled and poured into ice-cooled 1.5 M aq. HCl (2.0 L), ethyl acetate (1.0 L) was added and a white precipitate was formed. Additional ethyl acetate (5 L) was added to dissolve the solid, the phases were separated and the organic phase was washed with water (4 x 1 L) and evaporated. The residue (145 g) was suspended in MTBE (700 mL) and stirred at 50 °C for 30 min, then stirred at room temperature overnight. The solid was collected by suction filtration, washed with MTBE and dried to afford **6c** as a colorless solid (130 g, 90%). ¹H NMR (400 MHz, DMSO-*d*₆) δ 6.71 – 6.8 (m, 3H), 6.50 (d, *J* = 8.6 Hz, 1H),

5.17 (d, $J = 4.6$ Hz, 1H), 4.36 (t, $J = 4.9$ Hz, 1H), 4.19 (s, 4H), 3.43 – 3.54 (m, 1H), 1.31 (s, 9H), 0.93 (d, $J = 6.7$ Hz, 3H).

*Tert-butyl (1S,2R)-1-(2,3-dihydrobenzo[*b*][1,4]dioxin-6-yl)-1-hydroxypropan-2-ylcarbamate (ent-6c).* Following the procedures described for compound **6c** via **5c**, but starting from **ent-4**, afforded **ent-6c**. LCMS m/z 210 (MH^+ -BOC). 1H NMR (400 MHz, DMSO- d_6) δ 6.71 – 6.82 (m, 3H), 6.50 (d, $J = 8.6$ Hz, 1H), 5.17 (d, $J = 4.6$ Hz, 1H), 4.36 (t, $J = 4.8$ Hz, 1H), 4.19 (s, 4H), 3.42 – 3.54 (m, 1H), 1.31 (s, 9H), 0.93 (d, $J = 6.6$ Hz, 3H).

(1R,2S)-2-Amino-1-(3-methoxyphenyl)propan-1-ol hydrochloride (7b). Prepared as described for **7c**, starting from **6b** (16.1 g, 57.2 mmol) Yield: 11.4 g (92%) as a colorless salt. $[\alpha]_D^{20}$ -37.5° (c 1.0, MeOH). LCMS m/z 182 (MH^+). 1H NMR (600 MHz, DMSO- d_6) δ 8.18 (brs, 3H), 7.28 (t, $J = 7.9$ Hz, 1H), 6.89 – 6.95 (m, 2H), 6.81 – 6.87 (m, 1H), 6.04 (d, $J = 4.3$ Hz, 1H), 4.93 (t, $J = 3.3$ Hz, 1H), 3.75 (s, 3H), 3.3 – 3.43 (m, 1H), 0.94 (d, $J = 6.8$ Hz, 3H). ^{13}C NMR (151 MHz, DMSO- d_6) δ 159.20, 142.95, 129.28, 118.15, 112.69, 111.60, 71.22, 55.02, 51.77, 11.57. Chiral SFC (method C) $t_R = 0.97$ min, 99.6%. $t_R = 0.68$ min, 0.4% (1S,2R enantiomer). Chiral purity 99.2% ee.

*(1R,2S)-2-Amino-1-(2,3-dihydrobenzo[*b*][1,4]dioxin-6-yl)propan-1-ol hydrochloride (7c).* To a suspension of **6c** (129 g, 0.47 mol) in ethyl acetate (1050 mL) was added 6 N HCl in 2-propanol (250 mL, 1.5 mol). The mixture was stirred at 50 °C for 3 h and the resulting suspension was allowed to reach room temperature. The precipitate was filtered off, washed twice with ethyl acetate and dried under reduced pressure at 60 °C over night to afford **7c** as a colorless solid (80 g, 78%). $[\alpha]_D^{20}$ -39° (c 1.0, MeOH). Chiral purity, 99.4% ee, 100% de. LCMS m/z 210 (MH^+ -HCl). 1H NMR (400 MHz, DMSO- d_6) δ 7.95 (brs, 3H), 6.75 – 6.87 (m, 3H), 5.93 (d, $J = 4.2$ Hz, 1H), 4.77 (t, $J = 3.6$ Hz, 1H), 4.22 (s, 4H), 3.27 – 3.36 (m, 1H), 0.94 (d, $J = 6.7$ Hz, 3H). ^{13}C NMR (151 MHz, DMSO- d_6) δ C 143.07, 142.53, 134.27, 118.73,

116.74, 114.73, 70.89, 64.09, 64.03, 51.86, 11.67. Chiral SFC t_R = 2.15 min, 99%, t_R = 0.91 min, 0.3%, Chiral purity 99.4% ee, 100% de.

(1S,2R)-2-Amino-1-(2,3-dihydrobenzo[b][1,4]dioxin-6-yl)propan-1-ol hydrochloride

(**ent-7c**). Prepared essentially as described for **7c**, but starting from **ent-6c**. Yield 1.49 g (88%) of a colorless solid. $[\alpha]_D^{20} +37^\circ$ (c 1.0, MeOH). LCMS m/z 210 ($MH^+ - HCl$). 1H NMR (600 MHz, DMSO- d_6) δ 8.11 (brs, 3H), 6.76 – 6.87 (m, 3H), 5.94 (brd, J = 3.2 Hz, 1H), 4.8 – 4.86 (brm, 1H), 4.19 – 4.24 (brm, 4H), 3.21 – 3.34 (brm, 1H), 0.94 (d, J = 6.8 Hz, 3H). ^{13}C NMR (151 MHz, DMSO- d_6) δ 143.07, 142.54, 134.25, 118.73, 116.74, 114.73, 70.90, 64.08, 64.03, 51.83, 40.06, 11.69. Chiral SFC t_R = 0.91 min, 99.9%, t_R = 2.15 min. Chiral purity >99.9% ee. 100% de.

(4S,5R)-5-(2,3-Dihydrobenzo[b][1,4]dioxin-6-yl)-4-methyloxazolidin-2-one (8). A

suspension of **7c** (0.49 g, 1.99 mmol) and triethylamine (0.85 g, 1.2 mL, 8.39 mmol) in dry THF (35 mL) was cooled to $-30^\circ C$ and bis(trichloromethyl) carbonate (0.726 g, 2.45 mmol) in dry THF (5.0 mL) was slowly added. The reaction mixture was stirred at $-10^\circ C$ for 1 h and at room temperature for 1 h. To the suspension was added water (1 mL) and the mixture was evaporated. The residue was taken up in ethyl acetate (50 mL) and washed with aq. HCl (0.2 N) brine and sat. aq. bicarbonate. The organic phase was dried over anhydrous sodium sulfate, filtered and evaporated. The residue was purified by flash chromatography (ethyl acetate in heptane, 50-100%). The solvent was removed and the residue was taken up in a mixture of DCM and heptane. Evaporation afforded **8** as colorless solid (0.31 g, 66%). LCMS (ESI) m/z 236 (MH^+). 1H NMR (500 MHz, $CDCl_3$) δ 7.73 (s, 1H), 6.87 (d, J = 8.3 Hz, 1H), 6.7 – 6.78 (m, 2H), 5.55 (d, J = 8.0 Hz, 1H), 4.24 (s, 4H), 4.04 – 4.12 (m, 1H), 0.64 (d, J = 6.5 Hz, 3H). ^{13}C NMR (126 MHz, DMSO- d_6) δ 158.20, 143.12, 143.08, 128.96, 118.87, 116.94, 114.83, 79.03, 64.07, 64.03, 51.21, 17.01.

(4*S*,5*S*)-5-(2,3-Dihydrobenzo[*b*][1,4]dioxin-6-yl)-4-methyloxazolidin-2-one (**9**). To a solution of **6c** (2.00 g, 6.47 mmol) and triethylamine (0.99 mL, 7.11 mmol) in THF (24 mL) methanesulfonyl chloride (0.58 mL, 7.11 mmol) was added dropwise at 0 °C. The ice-cooled mixture was stirred for 30 min, thereafter stirring was continued at 50°C overnight. After addition of water (30 mL), the mixture was extracted with 3 portions of DCM and the organic phases were evaporated. The residue was purified by preparative HPLC (Kromasil KR-100-10-C18, 250 x 50 mm, 25-50% MeCN in water, 25 min) to yield **9** as a colorless solid (1.26 g, 83 %). LCMS *m/z* 236 (MH⁺). ¹H NMR (400 MHz, DMSO-*d*₆) δ 7.78 (s, 1H), 6.83 – 6.91 (m, 3H), 4.92 (d, *J* = 7.1 Hz, 1H), 4.24 (s, 4H), 3.66 (quint, *J* = 6.4 Hz, 1H), 1.18 (d, *J* = 6.1 Hz, 3H).

The assignment of the relative configuration of the diastereomers **8** and **9** is supported by the characteristic chemical shifts in the ¹H NMR for 2-CH₃ (**8**: δ 0.64; **9**: δ 1.18) and 5-H (**8**: δ 5.55; **9**: δ 4.92) which are in agreement with reported data.¹⁶

(4*R*,5*R*)-5-(2,3-Dihydrobenzo[*b*][1,4]dioxin-6-yl)-4-methyloxazolidin-2-one (**ent-9**). Prepared essentially as described for **9**, but starting from **ent-6c**. Yield: 1.73 g (68%) of a foamy solid. LCMS *m/z* 236 (MH⁺). ¹H NMR (400 MHz, DMSO-*d*₆) δ 7.78 (s, 1H), 6.83 – 6.91 (m, 3H), 4.92 (d, *J* = 7.1 Hz, 1H), 4.24 (s, 4H), 3.66 (quint, *J* = 6.3 Hz, 1H), 1.18 (d, *J* = 6.1 Hz, 3H).

(1*S*,2*S*)-2-Amino-1-(2,3-dihydrobenzo[*b*][1,4]dioxin-6-yl)propan-1-ol hydrochloride (**10**). To a solution of **9** (1.13 g, 4.82 mmol) in THF (10 mL) aq. LiOH (10 %, 15 mL, 62.7 mmol) was added and the mixture was stirred at 90 °C for 5h. Thereafter the mixture was allowed to reach room temperature, diluted with water and extracted with 3 portions of DCM. The combined organic phases were passed through a phase separator and evaporation of the solvent afforded the crude as an oil. The residue was taken up in DCM, HCl (1 M in diethylether) was added. After evaporation of the solvent a solid was obtained. Drying at

reduced pressure afforded **10** as a colorless solid (0.83 g, 70 %). LCMS m/z 210 ($MH^+ - HCl$). 1H NMR (400 MHz, DMSO- d_6) δ 7.91 (brs, 3H), 6.76 – 6.88 (m, 3H), 6.07 (d, J = 3.8 Hz, 1H), 4.32 (dd, J = 3.5, 8.6 Hz, 1H), 4.23 (s, 4H), 3.12 – 3.24 (m, 1H), 0.96 (d, J = 6.6 Hz, 3H).

*(1R,2R)-2-Amino-1-(2,3-dihydrobenzo[*b*][1,4]dioxin-6-yl)propan-1-ol hydrochloride (ent-10)*. Prepared essentially as described for **10**, but starting from **ent-9** (1.73 g, 7.36 mmol). Yield: 1.83 g (98%) of a colorless solid. LCMS m/z 210 ($MH^+ - HCl$). 1H NMR (400 MHz, DMSO- d_6) δ 7.88 (s, 3H), 6.78 – 6.89 (m, 3H), 6.08 (d, J = 3.8 Hz, 1H), 4.31 (dd, J = 3.7, 8.4 Hz, 1H), 4.23 (s, 4H), 3.12 – 3.25 (m, 1H), 0.96 (d, J = 6.6 Hz, 3H).

(1R,2S)-1-(1-(4-Fluorophenyl)-1H-indazol-5-yloxy)-1-(3-methoxyphenyl)propan-2-amine (11b). Prepared essentially as described for **12b**, starting from **7b** (0.5 g, 2.30 mmol) and **16** (0.93 g, 2.75 mmol). Yield (HCl salt): 0.47 g (47%) as a colorless solid. LCMS m/z 392 (MH^+). 1H NMR (500 MHz, MeOD) δ 8.03 (d, J = 0.9 Hz, 1H), 7.62 - 7.69 (m, 3H), 7.27 - 7.36 (m, 4H), 7.13 (d, J = 2.2 Hz, 1H), 6.99 - 7.03 (m, 2H), 6.92 (ddd, J = 8.3, 2.5, 0.7 Hz, 1H), 5.60 (d, J = 3.3 Hz, 1H), 3.79 - 3.83 (m, 1H), 3.78 (s, 3H), 1.33 (d, J = 6.8 Hz, 3H). ^{13}C NMR (126 MHz, MeOD) δ 162.70 (d, J = 245.3 Hz), 161.72, 153.74, 138.45, 137.47 (d, J = 2.9 Hz), 136.38, 135.97, 131.27, 126.67, 125.80 (d, J = 8.6 Hz), 121.12, 119.98, 117.35 (d, J = 23.2 Hz), 114.99, 113.70, 112.38, 105.51, 80.54, 55.75, 53.15, 13.19.

*Isobutyl 3-(5-((1R,2S)-2-amino-1-(2,3-dihydrobenzo[*b*][1,4]dioxin-6-yl)propoxy)-1H-indazol-1-yl)benzoate (12b)*. A mixture of **7c** (20.5 g, 83.3 mmol), 2-(dimethylamino)acetic acid (4.29 g, 41.6 mmol), cuprous iodide (3.97 g, 20.8 mmol) and cesium carbonate (84 g, 258 mmol) in butyronitrile (200 mL) was stirred and at 110 °C for 30 min. To that mixture a solution of **17** (35 g, 83.28 mmol) in butyronitrile (33 mL), generated by heating at 80 °C for 10 min, was added. The grayish reaction mixture was sealed and stirred at 110 °C for 19 h. To the cooled reaction mixture water and ethyl acetate (1.5 L) was added. The organic phase was

washed with water (3 x 700 mL). Evaporation of the solvents afforded of a gummy greenish residue (43 g). Purification by flash chromatography on silica gel, eluting with ethyl acetate in heptane (50-75-100%, containing 2% triethylamine), afforded **12b** (14 g, 34%) as a solid foam. LCMS m/z 502 (MH^+). HPLC t_R = 10.7 min, purity 97%. 1H NMR (400 MHz, DMSO- d_6) δ 8.25 (t, J = 1.9 Hz, 1H), 8.24 (d, J = 0.7 Hz, 1H), 8.05 (ddd, J = 0.9, 2.2, 8.1 Hz, 1H), 7.94 (dt, J = 1.1, 7.8 Hz, 1H), 7.69 – 7.77 (m, 2H), 7.22 (dd, J = 2.4, 9.1 Hz, 1H), 7.17 (d, J = 2.1 Hz, 1H), 6.85 – 6.91 (m, 2H), 6.81 (d, J = 8.2 Hz, 1H), 4.97 (d, J = 5.4 Hz, 1H), 4.19 (s, 4H), 4.12 (d, J = 6.5 Hz, 2H), 3.06 – 3.17 (m, 1H), 2 – 2.1 (m, 1H), 1.36 (brs, 2H), 1.07 (d, J = 6.4 Hz, 3H), 0.98 (d, J = 6.7 Hz, 6H).

Isobutyl 3-(5-((1R,2S)-2-(2,2-difluoropropanamido)-1-(2,3-dihydrobenzo[b][1,4]dioxin-6-yl)propoxy)-1H-indazol-1-yl)benzoate (13b). To an mixture of **12b** (3.95 g, 7.88 mmol) and 2,2-difluoropropanoic acid (1.25 g, 11.4 mmol) in DCM (40 mL) was added solid HATU (4.35 g, 11.5 mmol) and DIPEA (4.1 mL, 23.6 mmol). The mixture was stirred at room temperature for 2.5 h, the clear red solution obtained was washed with water, the water phase extracted once with DCM. The organic phases were further washed with water at pH=4 and at pH=8 and finally with brine and dried over $MgSO_4$. Removal of the solvents afforded a crude as a red sticky oil. Dissolving in DCM and purification by flash chromatography on silica (ethyl acetate in heptane, 0-50%) afforded **13b** (3.7 g, 79%) as a glassy solid. LCMS m/z 594 (MH^+), t_R = 2.77 min, 98%. 1H NMR (400 MHz, DMSO- d_6) δ 8.65 (d, J = 9.0 Hz, 1H), 8.26 (d, J = 0.7 Hz, 1H), 8.24 – 8.26 (m, 1H), 8.05 (ddd, J = 0.9, 2.2, 8.1 Hz, 1H), 7.95 (dt, J = 1.2, 7.9 Hz, 1H), 7.78 (d, J = 9.2 Hz, 1H), 7.73 (t, J = 7.9 Hz, 1H), 7.22 (dd, J = 2.4, 9.1 Hz, 1H), 7.14 (d, J = 2.2 Hz, 1H), 6.78 – 6.89 (m, 3H), 5.17 (d, J = 6.9 Hz, 1H), 4.14 – 4.23 (m, 5H), 4.12 (d, J = 6.5 Hz, 2H), 2 – 2.11 (m, 1H), 1.55 (t, J = 19.5 Hz, 3H), 1.29 (d, J = 6.8 Hz, 3H), 0.99 (d, J = 6.7 Hz, 6H).

3-(5-((1*R*,2*S*)-2-(2,2-Difluoropropanamido)-1-(2,3-dihydrobenzo[*b*][1,4]dioxin-6-yl)propoxy)-1*H*-indazol-1-yl)-*N*-((*S*)-tetrahydrofuran-3-yl)benzamide (**15l**). Following the procedure described for compound **15m** using **24b** (100 mg, 0.19 mmol) and (*S*)-tetrahydrofuran-3-amine hydrochloride (26 mg, 0.21 mmol) as starting materials. Yield: 85 mg (75%) as a colorless crystalline solid, mp = 175 °C. LCMS *m/z* 607 (MH⁺). HPLC *t*_R = 12.02 min, 99%. ¹H NMR (400 MHz, DMSO-*d*₆) δ 8.71 (d, *J* = 6.4 Hz, 1H), 8.65 (d, *J* = 8.5 Hz, 1H), 8.24 (d, *J* = 0.6 Hz, 1H), 8.18 (t, *J* = 1.7 Hz, 1H), 7.83 – 7.91 (m, 2H), 7.77 (d, *J* = 9.1 Hz, 1H), 7.65 (t, *J* = 7.9 Hz, 1H), 7.21 (dd, *J* = 2.3, 9.1 Hz, 1H), 7.13 (d, *J* = 2.2 Hz, 1H), 6.77 – 6.9 (m, 3H), 5.17 (d, *J* = 6.8 Hz, 1H), 4.44 – 4.52 (m, 1H), 4.11 – 4.23 (m, 5H), 3.8 – 3.91 (m, 2H), 3.66 – 3.77 (m, 1H), 3.61 (dd, *J* = 4.2, 8.9 Hz, 1H), 2.09 – 2.23 (m, 1H), 1.89 – 1.99 (m, 1H), 1.55 (t, *J* = 19.5 Hz, 3H), 1.29 (d, *J* = 6.8 Hz, 3H). Chiral HPLC (method A) *t*_R = 16.50 min, 98.7%. Chiral HPLC (method B) *t*_R = 25.67 min, 98.7%. Chiral HPLC (method C) *t*_R = 13.63 min, 100%. Chiral purity 100% ee, 97.8% de.

3-(5-((1*R*,2*S*)-2-(2,2-Difluoropropanamido)-1-(2,3-dihydrobenzo[*b*][1,4]dioxin-6-yl)propoxy)-1*H*-indazol-1-yl)-*N*-((*R*)-tetrahydrofuran-3-yl)benzamide (**15m**). A mixture of **24b** (100 mg, 0.19 mmol), (*R*)-tetrahydrofuran-3-amine 4-methylbenzenesulfonate (53 mg, 0.20 mmol) and HBTU (78 mg, 0.20 mmol) in DMF (2 mL) was treated with DIPEA (0.097 mL, 0.56 mmol). After stirred at room temperature for 1 h, the reaction mixture was diluted with water (2.5 mL) and MeCN (0.5 mL). The clear solution was purified by HPLC (Kromasil 100-10-C18, 50x250 mm, MeCN / water (0.1% TFA) 30-90%, 40 mL/min, 25 min). After freeze drying 109 mg of a glassy solid were obtained. After dissolving in warm ethyl acetate (3 mL) and addition of heptane (8 mL added in portions) a precipitate was formed. The suspension was stirred at room temperature for 20 h, the solid was collected by filtration, washed with a small volume of Heptane and dried at 40 °C under reduced pressure to afford the title compound **15m** as a colorless crystalline solid (88 mg, 78%), mp = 177 °C.

LCMS m/z 607 (MH^+). HPLC t_R = 12.03 min, 99%. 1H NMR (400 MHz, DMSO- d_6) δ 8.71 (d, J = 6.4 Hz, 1H), 8.65 (d, J = 8.7 Hz, 1H), 8.24 (s, 1H), 8.17 – 8.2 (m, 1H), 7.84 – 7.9 (m, 2H), 7.77 (d, J = 9.1 Hz, 1H), 7.65 (t, J = 7.9 Hz, 1H), 7.21 (dd, J = 2.3, 9.1 Hz, 1H), 7.14 (d, J = 2.1 Hz, 1H), 6.79 – 6.89 (m, 3H), 5.17 (d, J = 6.8 Hz, 1H), 4.44 – 4.53 (m, 1H), 4.11 – 4.24 (m, 5H), 3.82 – 3.9 (m, 2H), 3.72 (td, J = 6.0, 8.0 Hz, 1H), 3.61 (dd, J = 4.3, 8.9 Hz, 1H), 2.11 – 2.22 (m, 1H), 1.89 – 1.99 (m, 1H), 1.55 (t, J = 19.5 Hz, 3H), 1.30 (d, J = 6.7 Hz, 3H). ^{13}C NMR (100.6 MHz, DMSO- d_6) δ 165.58, 162.96 (t, J = 29.3 Hz), 152.96, 142.93, 142.85, 139.63, 135.74, 135.39, 133.93, 131.40, 129.60, 125.53, 125.26, 124.21, 120.58, 119.93, 119.62, 117.09 (t, J = 248.1 Hz), 116.80, 115.44, 111.58, 104.22, 81.10, 72.20, 66.49, 63.96, 63.93, 50.39, 50.00, 31.79, 21.00 (t, J = 25.4 Hz), 15.73. Chiral HPLC (method A) t_R = 19.18 min, 99.8%. Chiral HPLC (method B) t_R = 21.92 min, 99.8%. Chiral HPLC (method C) t_R = 13.26 min, 100%. Chiral purity 100% ee, 100% de.

1-(4-Fluorophenyl)-5-iodo-1H-indazole (**16**). A mixture of (4-fluorophenyl)hydrazine hydrochloride (29.8 g, 183 mmol) and 2-fluoro-5-iodobenzaldehyde (45.8 g, 183 mmol) in NMP (600 mL) was stirred at room temperature for 5 h. K_2CO_3 (76 g, 550 mmol) was added and the resulting suspension was stirred at 150 °C overnight. The mixture was cooled down to room temperature and poured into ice water (4 L), the resulting brown suspension was stirred overnight. A red brown solid was collected by filtration, washed with water and dried to leave a crude product (47 g). The crude was dissolved in DCM / heptane (1:1) and filtered through silica gel. The first fractions collected of red color were discarded and the succeeding yellow fractions were combined and concentrated to give a suspension. After addition of ethyl acetate and heptane the mixture was repeatedly concentrated and diluted with heptane. Collection of the precipitate by suction filtration yielded **16** as a yellow solid (20.9 g, 34%). LCMS m/z 339 (MH^+). 1H NMR (500 MHz, DMSO- d_6) δ 8.32 (d, J = 0.9 Hz, 1H), 8.31 (dd, J = 0.6, 1.6 Hz, 1H), 7.75 – 7.8 (m, 2H), 7.72 (dd, J = 1.6, 8.8 Hz, 1H), 7.63 (dt, J = 0.7, 8.9 Hz, 1H), 7.4 –

7.47 (m, 2H). ^{13}C NMR (126 MHz, DMSO- d_6) δ 160.52 (d, $J = 244.2$ Hz), 137.34, 135.62 (d, $J = 2.7$ Hz), 135.35, 134.71, 130.00, 127.37, 124.51 (d, $J = 8.6$ Hz), 116.49 (d, $J = 22.9$ Hz), 112.53, 85.41.

Isobutyl 3-(5-iodo-1H-indazol-1-yl)benzoate (17). Step 1. 2-fluoro-5-iodobenzaldehyde (5.12 g, 20.48 mmol), 3-hydrazinylbenzoic acid (3.22 g, 21.13 mmol) and Cs_2CO_3 (6.89 g, 21.13 mmol) in NMP (25 mL) was stirred at room temperature under argon atmosphere for 80 min. Water (100 mL) was added, the red solution was acidified with HCl (2 M, 25 mL), formed suspension was stirred for 15 min, solid collected by filtration, washed with water (3x) and dried at +50 °C under reduced pressure overnight to afford the intermediate hydrazone 3-(2-(2-Fluoro-5-iodobenzylidene)hydrazinyl)benzoic acid (**17a**) as a beige powder (80 wt-%, 9.35 g, 95%). ^1H NMR showed the presence of 20 wt-% NMP. ^1H NMR (400 MHz, DMSO- d_6) δ 12.88 (s, 1H), 10.86 (s, 1H), 8.17 (dd, $J = 2.1, 6.9$ Hz, 1H), 7.94 (s, 1H), 7.63 – 7.68 (m, 1H), 7.61 (s, 1H), 7.32 – 7.41 (m, 3H), 7.09 (dd, $J = 8.7, 10.7$ Hz, 1H). Step 2. **17a** (80 wt-%, 9.35 g, 19.5 mmol) dissolved in NMP (100 mL) was added potassium 2-methylpropan-2-olate (5.0 g, 44.9 mmol). The dark red solution was stirred at 160 °C for 30 min. The mixture was allowed to cool to room temperature, diluted with water (200 mL), acidified with HCl (2M, 25 mL) and extracted with EtOAc (3x 300 mL). The combined organic phases washed three times with water (3 x 400 mL). The organic phase were evaporated to afford 7.3 g of a brownish solid. Recrystallization from ethanol (50 mL) yielded the intermediate 3-(5-Iodo-1H-indazol-1-yl)benzoic acid (**17b**) (4.3 g, 60%) as a colorless solid. ^1H NMR (400 MHz, DMSO- d_6) δ 13.32 (s, 1H), 8.38 (d, $J = 0.8$ Hz, 1H), 8.34 (d, $J = 0.9$ Hz, 1H), 8.23 – 8.26 (m, 1H), 8.04 (ddd, $J = 1.0, 2.3, 8.0$ Hz, 1H), 7.97 (dt, $J = 1.2, 7.7$ Hz, 1H), 7.69 – 7.8 (m, 3H). Step 3. To a stirred mixture of **17b** (2.19 g, 6 mmol) and sodium carbonate (0.7 g, 6.6 mmol) in NMP (15 mL) at 40 °C was added 1-bromo-2-methylpropane (0.97 mL, 9.0 mmol) in one portion. After 1 hour, the temperature was raised to 55 °C and

another portion of 1-bromo-2-methylpropane (0.97 mL, 9.0 mmol) was added. The stirring was continued overnight. After cooling, the reaction mixture was partitioned between water and ethyl acetate. The organic phase was washed twice with water, dried over sodium sulfate, filtered and evaporated to dryness to afford **17** as a syrup that solidified to a beige material upon standing (2.5 g, 99 %). ^1H NMR (600 MHz, CDCl_3) δ 8.36 – 8.37 (m, 1H), 8.17 (d, J = 1.1 Hz, 1H), 8.14 (d, J = 0.7 Hz, 1H), 8.06 (dt, J = 7.8, 1.2 Hz, 1H), 7.91 (ddd, J = 8.0, 2.2, 1.0 Hz, 1H), 7.68 (dd, J = 8.8, 1.6 Hz, 1H), 7.63 (t, J = 7.9 Hz, 1H), 7.55 (d, J = 8.8 Hz, 1H), 4.16 (d, J = 6.7 Hz, 2H), 2.07 – 2.16 (m, 1H), 1.04 (d, J = 6.8 Hz, 6H). ^{13}C NMR (151 MHz, CDCl_3) δ 165.84, 140.08, 137.95, 135.87, 134.87, 132.14, 130.49, 129.89, 128.00, 127.98, 127.02, 123.31, 112.18, 85.10, 71.56, 28.02, 19.35.

3-(5-((1*R*,2*S*)-2-(2,2-Difluoropropanamido)-1-(2,3-dihydrobenzo[*b*][1,4]dioxin-6-yl)propoxy)-1*H*-indazol-1-yl)benzoic acid (**24b**). To a solution of **13b** (3.67 g, 6.18 mmol) THF (15 mL) and MeOH (15 mL) was added 2.0 M LiOH solution in water (6.1 mL, 12.4 mmol). After stirring for 3 h the reaction mixture was poured into water (400 mL), cooled in an ice water bath and acidified to pH 2 by slow addition of 1 M HCl while stirring. A solid precipitated was collected by filtration, washed with 0.1 M HCl (50 mL), water (100 mL) and dried at reduced pressure. In order to remove hydrolyzed amide, the solid was re-dissolved in a mixture of MeOH:water:AcOH (90:10:10, 150 mL) and filtered through an 10g ISOLUTE-SCX column. The slightly yellow solution was concentrated to about 25 mL and diluted with water (400 mL), the pH was adjusted to pH=2 by addition of 1M HCl. The suspension was stirred for 30 min, the solid was filtered off, washed with water and dried under reduced pressure at 40°C to afford **24b** as a slightly yellow solid (2.9 g, 87%). LCMS m/z 538 (MH^+). HPLC t_R = 12.55 min, 97%. ^1H NMR (400 MHz, $\text{DMSO}-d_6$) δ 13.27 (s, 1H), 8.65 (d, J = 8.7 Hz, 1H), 8.25 (d, J = 0.7 Hz, 1H), 8.21 – 8.23 (m, 1H), 8.00 (ddd, J = 1.0, 2.3, 8.1 Hz, 1H), 7.92 (dt, J = 1.2, 7.8 Hz, 1H), 7.77 (d, J = 9.1 Hz, 1H), 7.69 (t, J = 7.9 Hz, 1H), 7.22 (dd, J =

2.3, 9.1 Hz, 1H), 7.14 (d, $J = 2.2$ Hz, 1H), 6.79 – 6.89 (m, 3H), 5.17 (d, $J = 6.8$ Hz, 1H), 4.11 – 4.23 (m, 5H), 1.55 (t, $J = 19.5$ Hz, 3H), 1.29 (d, $J = 6.7$ Hz, 3H). ^{13}C NMR (100.6 MHz, DMSO- d_6) δ 166.64, 162.98 (t, $J = 29.0$ Hz), 153.01, 142.95, 142.88, 139.90, 135.68, 133.82, 132.30, 131.39, 130.08, 126.81, 125.70, 125.39, 121.93, 120.06, 119.65, 117.10 (t, $J = 248.2$ Hz), 116.81, 115.46, 111.47, 104.31, 81.10, 63.98, 63.94, 50.01, 21.01 (t, $J = 25.4$ Hz), 15.76.

ASSOCIATED CONTENT

Supplementary Information

Chemistry: additional synthetic procedures and analytical data; X-ray structure determination; *in vitro* pharmacology; dry powder inhalation protocol; protocol for pharmacokinetic studies in rat; rat Sephadex model: protocol and raw data; cross-species *in vitro* metabolism: protocols and schemes (PDF). Molecular formula strings (CSV).

AUTHOR INFORMATION

Corresponding author

E-mail: martin.hemmerling@astrazeneca.com

ACKNOWLEDGMENTS

The authors like to thank Göran Carlström for NMR-support, Marianne Juhlin, Inger Remse and Charlotte Kåse for contributions to *in vitro* pharmacology, Mikael Lundqvist, Ann Tjörnebo, Gösta Hallström and Karin Sjödin for their contributions to the metabolite identification studies, Cristian Bodin and Hongwei Guo for experimental contribution experimental contributions to protein crystallization.

ABBREVIATIONS USED

APCI, atmospheric-pressure chemical ionization; AR, androgen receptor; Chrom logD, logD by HPLC method; CL_{int}, intrinsic clearance; COPD, chronic obstructive pulmonary disease; DIPEA, *N,N*-diisopropylethylamine; DPI, dry powder inhalation; ER, estrogen receptor; F, oral bioavailability; FF, fluticasone furoate; GR, glucocorticoid receptor; HATU, 1-[Bis(dimethylamino)methylene]-1*H*-1,2,3-triazolo[4,5-*b*]pyridinium 3-oxid hexafluorophosphate; HBTU, 2-(1*H*-benzotriazol-1-yl)-1,1,3,3-tetramethyluronium hexafluorophosphate; ICS, inhaled corticosteroid; *it*, intratracheal; *iv*, intravenous; LBD, ligand binding domain; LPS, lipopolysaccharide; MR, mineralocorticoid receptor; MRT, mean retention time; PBMC, peripheral blood mononuclear cell; p.o., PR, progesterone receptor; TNF, tumor necrosis factor; TR, therapeutic ratio; T3P, propanephosphonic acid; XRPD, X-ray powder diagram.

PDB ID codes: 5NFP (compound **2**); 5NFT (compound **1b**). Authors will release the atomic coordinates and experimental data upon article publication.

REFERENCES

1. Hirschmann, R. Medicinal chemistry in the golden age of biology: lessons from steroid and peptide research. *Angew. Chem. Int. Ed.* **1991**, *30*, 1278-1301.
2. Barnes, P. J. Glucocorticosteroids: current and future directions. *Br. J. Pharmacol.* **2011**, *163*, 29-43.
3. (a) Goulding, N. J. The molecular complexity of glucocorticoid actions in inflammation - a four-ring circus. *Curr. Opin. Pharmacol.* **2004**, *4*, 629-636; (b) Barnes, P. J. Molecular mechanisms and cellular effects of glucocorticosteroids. *Immunol. Allergy Clin. North Am.* **2005**, *25*, 451-468; (c) Weikum, E. R.; Knuesel, M. T.; Ortlund, E. A.; Yamamoto, K. R. Glucocorticoid receptor control of

- transcription: precision and plasticity via allostery. *Nat. Rev. Mol. Cell Biol.* **2017**, *18*, 159-174.
4. Fardet, L.; Feve, B. Systemic glucocorticoid therapy: a review of its metabolic and cardiovascular adverse events. *Drugs* **2014**, *74*, 1731-1745.
5. Uings, I. J.; Farrow, S. N. A pharmacological approach to enhancing the therapeutic index of corticosteroids in airway inflammatory disease. *Curr. Opin. Pharmacol.* **2005**, *5*, 221-226.
6. White, M.; Crisalida, T.; Li, H.; Economides, A.; Kaliner, M. Effects of long-term inhaled corticosteroids on adrenal function in patients with asthma. *Ann. Allergy, Asthma, Immunol.* **2006**, *96*, 437-444.
7. (a) Allen, D. B.; Bielory, L.; Derendorf, H.; Dluhy, R.; Colice, G. L.; Szeffler, S. J. Inhaled corticosteroids: past lessons and future issues. *J. Allergy Clin. Immunol.* **2003**, *112*, S1-40; (b) Pruteanu, A. I.; Chauhan, B. F.; Zhang, L.; Prietsch, S. O. M.; Ducharme, F. M. Inhaled corticosteroids in children with persistent asthma: is there a dose response impact on growth? An overview of Cochrane reviews. *Paediatr. Respir. Rev.* **2015**, *16*, 51-52; (c) Rossi, A. P.; Zanardi, E.; Zamboni, M.; Rossi, A. Optimizing treatment of elderly COPD patients: what role for inhaled corticosteroids? *Drugs Aging* **2015**, *32*, 679-687.
8. Barnes, P. J. Corticosteroid resistance in patients with asthma and chronic obstructive pulmonary disease. *J. Allergy Clin. Immunol.* **2013**, *131*, 636-645.
9. Hemmerling, M.; Edman, K.; Lepisto, M.; Eriksson, A.; Ivanova, S.; Dahmen, J.; Rehwinkel, H.; Berger, M.; Hendrickx, R.; Dearman, M.; Jensen, T. J.; Wissler, L.;

- Hansson, T. Discovery of indazole ethers as novel, potent, non-steroidal glucocorticoid receptor modulators. *Bioorg. Med. Chem. Lett.* **2016**, *26*, 5741-5748.
10. (a) Biggadike, K.; Uings, I.; Farrow, S. N. Designing corticosteroid drugs for pulmonary selectivity. *Proc. Am. Thorac. Soc.* **2004**, *1*, 352-355; (b) Millan, D. S.; Bunnage, M. E.; Burrows, J. L.; Butcher, K. J.; Dodd, P. G.; Evans, T. J.; Fairman, D. A.; Hughes, S. J.; Kilty, I. C.; Lemaitre, A.; Lewthwaite, R. A.; Mahnke, A.; Mathias, J. P.; Philip, J.; Smith, R. T.; Stefaniak, M. H.; Yeadon, M.; Phillips, C. Design and synthesis of inhaled p38 inhibitors for the treatment of chronic obstructive pulmonary disease. *J. Med. Chem.* **2011**, *54*, 7797-7814; (c) Cooper, A. E.; Ferguson, D.; Grime, K. Optimisation of DMPK by the inhaled route: challenges and approaches. *Curr. Drug Metab.* **2012**, *13*, 457-473; (d) Tayab, Z. R.; Hochhaus, G. Pharmacokinetic/pharmacodynamic evaluation of inhalation drugs: application to targeted pulmonary delivery systems. *Expert Opin. Drug Delivery* **2005**, *2*, 519-532.
11. Claus, S.; Weiler, C.; Schiewe, J.; Friess, W. How can we bring high drug doses to the lung? *Eur. J. Pharm. Biopharm.* **2014**, *86*, 1-6.
12. (a) Wu, K.; Blomgren, A. L.; Ekholm, K.; Weber, B.; Edsbaecker, S.; Hochhaus, G. Budesonide and ciclesonide: effect of tissue binding on pulmonary receptor binding. *Drug Metab. Dispos.* **2009**, *37*, 1421-1426; (b) Schmidt, S.; Gonzalez, D.; Derendorf, H. Significance of protein binding in pharmacokinetics and pharmacodynamics. *J. Pharm. Sci.* **2010**, *99*, 1107-1122.
13. Belvisi, M. G.; Bundschuh, D. S.; Stoeck, M.; Wicks, S.; Underwood, S.; Battram, C. H.; Haddad el, B.; Webber, S. E.; Foster, M. L. Preclinical profile of ciclesonide, a novel corticosteroid for the treatment of asthma. *J. Pharmacol. Exp. Ther.* **2005**, *314*, 568-574.

- 1
2
3 14. Conrad, K.; Hsiao, Y.; Miller, R. A practical one-pot process for α -amino aryl ketone
4 synthesis. *Tetrahedron Lett.* **2005**, *46*, 8587-8589.
5
6
7
8 15. Yin, J.; Huffman, M. A.; Conrad, K. M.; Armstrong, J. D. 3rd. Highly
9 diastereoselective catalytic Meerwein-Ponndorf-Verley reductions. *J. Org. Chem.*
10 **2006**, *71*, 840-843.
11
12
13
14 16. Davies, S. G.; Doisneau, G. J.-M. Base induced C-5 epimerisation of 4-methyl-5-
15 phenyl oxazolidinones: chiral auxiliaries derived from norephedrine and
16 norpseudoephedrine. *Tetrahedron: Asymmetry* **1993**, *4*, 2513-2516.
17
18
19
20 17. Job, G. E.; Buchwald, S. L. Copper-catalyzed arylation of beta-amino alcohols. *Org.*
21 *Lett.* **2002**, *4*, 3703-3706.
22
23
24
25 18. (a) Edsbacker, S.; Jonsson, S.; Lindberg, C.; Ryrfeldt, A.; Thalen, A. Metabolic
26 pathways of the topical glucocorticoid budesonide in man. *Drug Metab. Dispos.*
27 **1983**, *11*, 590-596; (b) Hughes, S. C.; Shardlow, P. C.; Hollis, F. J.; Scott, R. J.;
28 Motivaras, D. S.; Allen, A.; Rousell, V. M. Metabolism and disposition of
29 fluticasone furoate, an enhanced-affinity glucocorticoid, in humans. *Drug Metab.*
30 *Dispos.* **2008**, *36*, 2337-2344.
31
32
33
34
35 19. Jacobson, L.; Middleton, B.; Holmgren, J.; Eirefelt, S.; Frojd, M.; Blomgren, A.;
36 Gustavsson, L. An optimized automated assay for determination of metabolic
37 stability using hepatocytes: assay validation, variance component analysis, and in
38 vivo relevance. *Assay Drug Dev. Technol.* **2007**, *5*, 403-415.
39
40
41
42
43 20. Sellers, S.; Horodnik, W.; House, A.; Wylie, J.; Mauser, P.; Donovan, B. The in vitro
44 and in vivo investigation of a novel small chamber dry powder inhalation delivery
45 system for preclinical dosing to rats. *Inhalation Toxicol.* **2015**, *27*, 706-716.
46
47
48
49
50
51
52
53
54
55
56
57
58
59
60

- 1
2
3 21. Valotis, A.; Hogger, P. Human receptor kinetics and lung tissue retention of the
4 enhanced-affinity glucocorticoid fluticasone furoate. *Respir. Res.* **2007**, *8*, 54.
5
6
7
8 22. (a) Kallstrom, L.; Brattsand, R.; Lovgren, U.; Svensjo, E.; Roempke, K. A rat model
9 for testing anti-inflammatory action in lung and the effect of glucocorticosteroids
10 (GCS) in this model. *Agents Actions* **1986**, *17*, 355-357; (b) Kubin, R.; Deschl, U.;
11 Linssen, M.; Wilhelms, O. H. Intratracheal application of Sephadex in rats leads to
12 massive pulmonary eosinophilia without bronchial hyperreactivity to acetylcholine.
13 *Int. Arch. Allergy Immunol.* **1992**, *98*, 266-272.
14
15
16
17
18
19
20
21
22 23. (a) Gomez-Sanchez, C. E. Glucocorticoid production and regulation in thymus: of
23 mice and birds. *Endocrinology* **2009**, *150*, 3977-3979; (b) Bar-Dayana, Y.; Afek, A.;
24 Bar-Dayana, Y.; Goldberg, I.; Kopolovic, J. Proliferation, apoptosis and thymic
25 involution. *Tissue Cell* **1999**, *31*, 391-396; (c) Vacchio, M. S.; Ashwell, J. D.
26 Glucocorticoids and thymocyte development. *Semin. Immunol.* **2000**, *12*, 475-485.
27
28
29
30
31
32
33
34 24. (a) Gauvreau, G. M.; Boulet, L. P.; Leigh, R.; Cockcroft, D. W.; Killian, K. J.; Davis,
35 B. E.; Deschesnes, F.; Watson, R. M.; Swystun, V.; Mardh, C. K.; Wessman, P.;
36 Jorup, C.; Aurivillius, M.; O'Byrne, P. M. A nonsteroidal glucocorticoid receptor
37 agonist inhibits allergen-induced late asthmatic responses. *Am. J. Respir. Crit. Care*
38 *Med.* **2015**, *191*, 161-167. (b) Berger, M.; Dahmen, J.; Eriksson, A.; Gabos, B.;
39 Hansson, T.; Hemmerling, M.; Henriksson, K.; Ivanova, S.; Lepistoe, M.;
40 McKerrecher, D.; Munck Af Rosenschoeld, M.; Nilsson, S.; Rehwinkel, H.; Taflin,
41 C. Indazolyl ester and amide derivatives for the treatment of glucocorticoid receptor
42 mediated disorders and their preparation. WO 2008076048, June 26, 2008.
43
44
45
46
47
48
49
50
51
52
53
54
55 25. (a) Edman, K.; Ahlgren, R.; Bengtsson, M.; Bladh, H.; Backstrom, S.; Dahmen, J.;
56 Henriksson, K.; Hillertz, P.; Hulikal, V.; Jerre, A.; Kinchin, L.; Kase, C.; Lepisto,
57
58
59
60

- M.; Mile, I.; Nilsson, S.; Smailagic, A.; Taylor, J.; Tjornebo, A.; Wissler, L.; Hansson, T. The discovery of potent and selective non-steroidal glucocorticoid receptor modulators, suitable for inhalation. *Bioorg. Med. Chem. Lett.* **2014**, *24*, 2571-2577; (b) Sheppeck, J. E., 2nd; Gilmore, J. L.; Xiao, H. Y.; Dhar, T. G.; Nirschl, D.; Doweyko, A. M.; Sack, J. S.; Corbett, M. J.; Malley, M. F.; Gougoutas, J. Z.; McKay, L.; Cunningham, M. D.; Habte, S. F.; Dodd, J. H.; Nadler, S. G.; Somerville, J. E.; Barrish, J. C. Discovery of potent and selective nonsteroidal indazolyl amide glucocorticoid receptor agonists. *Bioorg. Med. Chem. Lett.* **2013**, *23*, 5442-5447; (c) Yates, C. M.; Brown, P. J.; Stewart, E. L.; Patten, C.; Austin, R. J.; Holt, J. A.; Maglich, J. M.; Angell, D. C.; Sasse, R. Z.; Taylor, S. J.; Uings, I. J.; Trump, R. P. Structure guided design of 5-arylindazole glucocorticoid receptor agonists and antagonists. *J. Med. Chem.* **2010**, *53*, 4531-4544; (d) Biggadike, K.; Bledsoe, R. K.; Coe, D. M.; Cooper, T. W.; House, D.; Iannone, M. A.; Macdonald, S. J.; Madauss, K. P.; McLay, I. M.; Shipley, T. J.; Taylor, S. J.; Tran, T. B.; Uings, I. J.; Weller, V.; Williams, S. P. Design and x-ray crystal structures of high-potency nonsteroidal glucocorticoid agonists exploiting a novel binding site on the receptor. *Proc. Nat. Acad. Sci. U. S. A.* **2009**, *106*, 18114-18119.
26. (a) Salter, M.; Biggadike, K.; Matthews, J. L.; West, M. R.; Haase, M. V.; Farrow, S. N.; Uings, I. J.; Gray, D. W. Pharmacological properties of the enhanced-affinity glucocorticoid fluticasone furoate in vitro and in an in vivo model of respiratory inflammatory disease. *Am. J. Physiol. Lung Cell. Mol. Physiol.* **2007**, *293*, L660-667; (b) Grossmann, C.; Scholz, T.; Rochel, M.; Bumke-Vogt, C.; Oelkers, W.; Pfeiffer, A. F.; Diederich, S.; Bahr, V. Transactivation via the human glucocorticoid and mineralocorticoid receptor by therapeutically used steroids in CV-1 cells: a

- comparison of their glucocorticoid and mineralocorticoid properties. *Eur. J. Endocrinol.* **2004**, *151*, 397-406.
27. Boger, E.; Evans, N.; Chappell, M.; Lundqvist, A.; Ewing, P.; Wigenborg, A.; Friden, M. Systems pharmacology approach for prediction of pulmonary and systemic pharmacokinetics and receptor occupancy of inhaled drugs. *CPT Pharmacometrics Syst. Pharmacol.* **2016**, *5*, 201-210.
28. Berger, M.; Dahmen, J.; Edman, K.; Eriksson, A.; Hansson, T.; Hemmerling, M.; Hossain, N.; Klingstedt, T.; Lepistö, M.; Nilsson, S.; Rehwinkel, H. Phenyl and benzodioxinyl substituted indazole derivatives. WO 2009142571, November 26, 2009.
29. Kuna, P.; Aurivillius, M.; Jorup, C.; Prothon, S.; Taib, Z.; Edsbacker, S. Efficacy and tolerability of an inhaled selective glucocorticoid receptor modulator - AZD5423 - in COPD patients: Phase II Study Results. *Basic Clin. Pharmacol. Toxicol.* [Online early access]. DOI:10.1111/bcpt.12768. July 17, 2017. <http://dx.doi.org/10.1111/bcpt.12768> (accessed September 14, 2017).
30. ClinicalTrials.gov identifier: NCT02479412. A multiple dosing (14 days) study to assess efficacy and safety of three dose levels of AZD7594, given once daily by inhalation, in patients with mild to moderate asthma. <https://clinicaltrials.gov/show/NCT02479412> (accessed September 13, 2017).

Table of Contents Graphic

